Throughput Improvements for FHMA Wireless Data Networks Employing Variable Rate Channel Coding

by

Andrew S. Park

Report submitted to the faculty of the

Virginia Polytechnic Institute and State University

in partial fulfillment of the requirements for the degree of

MASTER OF SCIENCE

in

Electrical Engineering

APPROVED:

Dr. Brian D. Woerner, Chairman

Dr. Theodore Rappaport

Dr. Gail Gray

DEC, 1996

Blacksburg, Virginia

Keywords: Frequency hopping, FHMA, Variable Rate Coding, Channel Coding

Throughput Improvements for FHMA Wireless Data Networks Employing Variable Rate Channel Coding

by

Andrew S. Park

Committee Chairman: Dr. Brian D. Woerner

Bradley Department of Electrical Engineering

(ABSTRACT)

The increasing need for secure, high throughput wireless data networks has led to a search for spectrally efficient wireless systems which make better use of the available bandwidth. We propose that greater spectral efficiency can be achieved in Frequency Hopped Multiple Access (FHMA) networks by improving the coding efficiency of these systems through a technique called Variable Rate Coding (VRC). With VRC, an adaptable code rate is employed during communication allowing a transmitter-receiver pair to adapt the amount of redundancy provided by an error correction code to the quality of the channel. This is opposed to a Fixed Rate Coding (FRC) scheme in which a fixed code rate is utilized to provide sufficient protection for the worst case channel conditions. If the quality of the channel can be accurately estimated during communication, we show that VRC can provide significant throughput advantages over traditional FRC schemes for non-orthogonally hopped FHMA networks.

ACKNOWLEDGEMENTS

I thank Dr. Brian D. Woerner for his guidance, direction, and generous funding as my advisor throughout my graduate career. I also thank Dr. Mike Buehrer whose friendship and mentoring were invaluable to me while he was here.

I would also like to thank Global-Net, General Motors, and the National Science Foundation for the financial assistance and scholarships they provided during portions of my education. I would also like to thank Loretta Estes for her always patient and kind advice during my graduate studies.

I am grateful to every member of the Mobile and Portable Radio Research Group (MPRG) who assisted me through different stages of my research. Special thanks are due to Nitin Mangalvedhe and Paul Petrus for their frequent help with all types of problems.

Finally I dedicate this work to Jesus Christ to whom I've pledged my life, and also to my loving (and lovable) wife Tara. I thank my parents, Thae Soo and Youngmee Park, as well as my inlaws Carol Ann and Johnny Manese who always gave me mountains of support during my graduate studies.

TABLE OF CONTENTS

LIST OF FIGURES

Chapter 1

Introduction

Since the FCC began auctioning bandwidth for wireless services in 1994, billions of dollars have been raised for the U.S. Treasury [1]. The magnitude of money pledged by current and would-be wireless communications service providers is a hint of the accelerating demand for wireless communication services. In the 1990's the paging and cellular industries have experienced annual growth rates of 40% in the U.S. [2] with some analysts predicting 50 to 100 million subscribers in the U.S. alone by the turn of the century [3]. Demand for digital Personal Communications Services (PCS) which can provide integrated voice and data services has spurred rapid deployment of new digital technologies and standards such as the Global System for Mobile Communications (GSM) standard and Qualcomm's IS-95 Code Division Multiple Access (CDMA) standard. Demand for mobile data networks in hospitals, warehouses, and corporate offices has led to the recent IEEE 802.11 standard and skyrocketing revenues for Wireless LAN manufacturers such as Proxim. And the tremendous worldwide market for Wireless Local Loop (WLL) systems has encouraged a plethora of promising WLL products and standards from wireless equipment manufacturers and technology developers such as DSC, Qualcomm, and Interdigital.

In coming years, the proliferation of wireless applications will cause the available bandwidth for such services to become increasingly valuable. For this reason, there has been a search for spectrally efficient wireless systems which make better use of the available bandwidth. This search has created a particular interest in Spread Spectrum (SS) systems which can offer significant capacity improvements in multi-cell systems. A great deal of emphasis has been placed on Direct Sequence Spread Spectrum (DS/SS) [4] [5] particularly in PCS systems, first generation Wireless LANs, and WLL systems. But another wireless network

technology, Frequency Hopped Multiple Access (FHMA), which uses Frequency Hopped Spread Spectrum (FH/SS) has become widely used in military packet radio networks for several years. One example of a wireless military network employing FH/SS is the Single Channel Ground and Airborne Radio System (SINCGARS) system[1], the current standard combat net radio for the U.S. Army and Marine Corps. The SINCGARS' FH/SS technology allowed it to be the only combat net radio that could not be jammed by hostile forces in the 1991 Middle East conflict. In addition to its popularity in military wireless networks, FH/SS has recently also found commercial use in the GSM standard [6] [7], the Cellular Digital Packet Data (CDPD) standard, second generation Wireless LANs, the Geotek Specialized Mobile Radio (SMR) voice/data network, and in a plethora of low power unlicensed systems [8].

[1]The latest generation, the SINCGARS TCS adds data communications to the SINCGARS system.

1.1 Frequency Hopping

FH/SS provides several advantages over non-hopped narrowband systems including:

1: *FH/SS provides a form of frequency diversity resulting in better performance in a slow fading environment [9].*

2: *FH/SS provides interference diversity nearly eliminating the possibility of a single rogue user disrupting the entire system or making the system unusable for any given user in the system.*

3: *FH/SS provides a high level of security due to the pseudorandom hopping patterns employed by the users.*

FH/SS also provides several advantages over DS/SS wideband systems including:

1: *FH/SS is naturally more resistant to the near/far problem than is DS/SS making FH/SS more practical than DS/SS for decentralized networks.*

2: *FH/SS can aggregate discontiguous blocks of spectrum thus affording greater flexibility in spectrum management. This is in contrast to DS/SS which requires a contiguous block of spectrum.*

3: *The synchronization requirements for FH/SS are generally less stringent than DS/SS.*

Efforts to increase the capacity of wireless networks have led to heavy research in technologies such as smart antennas [10] [11] and interference rejection [12] [13] which can increase system capacity by reducing the effects of interference at the receiver. This thesis proposes that another technique, Variable Rate Coding (VRC), which adapts the code rate of an error correction code to the quality of the channel can improve the spectral efficiency of a FHMA system thereby increasing system capacity[2]. In particular, we present an analysis of the potential throughput gains provided by a VRC scheme which uses an adaptable

[2]We do not mean to suggest that Variable Rate Coding is limited to FHMA applications. The idea of Variable Rate Coding can be explored for application to any digital communication system to achieve greater

code rate R_{var} rather than a single fixed code rate R_{fix} which is designed for the worst case channel conditions. Fixed Rate Coding (FRC) schemes are designed to provide sufficient error correction for the worst case channel conditions to avoid the severe performance degradation which can occur if the error correction capability of the code is exceeded.

---

spectral efficiency. Our analysis in this thesis however is limited in scope to FHMA systems but we believe the results can give an first order intuitive feel for the magnitude of capacity gains possible for other types of systems.

1.2 Contribution of This Thesis

This thesis builds upon work of several previous research efforts. Work done by Kim and Stark [14] [15] examined performance bounds for FRC schemes as well as optimal code rates for very long Reed-Solomon (RS) error correction codes. The idea of Variable Rate Coding (VRC) was first proposed in by A.I. Wardhana and B.D. Woerner in [16] where it was suggested that VRC could provide throughput gains in FHMA systems employing non-orthogonal hopping patterns. In this thesis, we build upon the work in [14] and [15] by considering performance bounds of practical length RS FRC schemes for FHMA systems. We also build upon the work in [16] by undertaking a more rigorous analysis of the idea of VRC and presenting comparative results under a variety of system conditions and configurations. Synchronous and asynchronous hopped systems are examined with and without the availability of side information (i.e., information on when "collisions" occur during system operation between two or more hopping users).

In particular, we intend to quantify the magnitude of the performance gains possible with a VRC scheme in FHMA systems and the requirements to achieve these gains. VRC implementations with theoretical perfect codes (i.e., codes which achieve channel capacity) as well as practical length Reed-Solomon codes are examined and performance comparisons are made against various FRC designs.

VRC can provide an effective method for increasing the capacity of many wireless data systems without requiring additional bandwidth. This could be a tremendous advantage for future wireless systems which will almost certainly be capacity limited due to rapidly growing demand for mobile voice and data services as well as the likelihood of future multimedia applications which require high data throughputs. Possible applications of VRC in FHMA systems could be Wireless LANs, wireless Internet Personal Digital Assistants (PDAs), future generations for the SINCGARS TCS [3] system, or future military wireless ATM (Asynchronous Transfer Mode) networks [4]. In any of these applications, VRC could

[3]The SINCGARS TCS system is a version of SINCGARS which includes data communications capabilities

[4]Recently, there has been an increasing amount of interest by the U.S. military in highly secure wireless

potentially improve throughput performance and allow a larger bit pipe (on average) for advanced high bit rate applications. VRC would most likely be best suited to cases where the channel quality does not change so quickly that an adaptable code rate scheme becomes impractical. In non-orthogonally hopped FHMA systems where the channel quality is largely determined by the number of users in the system (rather than fast fading effects), VRC may be a viable and effective way of increasing throughput.

ATM networks which would be able to provide real-time maps, photographs, and other battle information to ground forces during combat.

1.3 Organization of Thesis

Chapter 2 provides an overview of spread spectrum and FHMA specific concepts and terms. The two major classes of spread spectrum, Direct Sequence Spread Spectrum (DS/SS) and Frequency Hopped Spread Spectrum (FH/SS), are introduced and explained. Chapter 3 contains the basic error correction coding theory necessary to understand the contents of this thesis. Two major classes of error correction codes (i.e., "convolutional codes" and "block codes") are introduced as well as important coding theory terms and concepts such as *minimum distance* and *code rate*. Chapter 4 presents the idea of VRC in detail and explains how VRC can provide superior throughput compared to realistic FRC schemes. VRC's compatibility to other throughput improving (or capacity improving) technologies for wireless networks is also briefly described in chapter 4. Chapters 5 presents results of the analysis including throughput results for optimal VRC and optimal FRC schemes, comparisons between VRC and FRC throughputs, and an analysis of the performance degradation of both VRC and FRC schemes in a Rayleigh flat fading environment. Finally, Chapter 6 summarizes the work contained in this thesis and outlines future research on this topic.

Chapter 2

Spread Spectrum

Recently, many wireless systems have been moving towards spread spectrum techniques from traditional narrowband transmission techniques. Some examples of wireless systems using spread spectrum techniques include the GSM digital cellular standard, the IS-95 CDMA standard, and the U.S. military's SINCGARS communications network. The two most common forms of spread spectrum are Direct Sequence Spread Spectrum (DS/SS) and Frequency Hopped Spread Spectrum (FH/SS).

The GSM standard employs FH/SS as an option to allow GSM carriers (with up to 8 time division multiplexed users each) to average the interference on several channels. Some manufacturers of GSM equipment claim that frequency hopping can improve overall Carrier to Interference ratios (i.e., C/I) by around 2 dB in some cases.

The IS-95 standard employs DS/SS and Code Division Multiple Access techniques to provide significant capacity gains when compared to traditional narrowband transmission techniques [5]. The capacity increases that IS-95 promises has lured many U.S. PCS service providers in 1995 to commit to deploying this new (and relatively unproven) technology in order to ably compete with traditional analog cellular services.

The U.S. military's SINCGARS combat net radio employs FH/SS to provide an anti-jamming capability that has consistently performed well beyond U.S. Army specifications under combat conditions in the Desert Shield/Desert Storm conflict as well as in the Korean demilitarized zone.

The reasons why spread spectrum is used in a particular system can vary according to the requirements of the network as well as the propagation environment. In addition to providing the benefits mentioned above, spread spectrum techniques can also offer other

attractive properties depending on the particular implementation considered.

2.1 Definition of Spread Spectrum

"Spread Spectrum" refers to a system which satisfies three basic conditions [17]. These three conditions are:

1: *The carrier signal occupies a bandwidth much larger than* $1/T_s$ *where* T_s *is the message symbol duration.*

2: *The signal is pseudorandom (i.e., the signal appears to be unpredictable).*

3: *Reception of the signal is accomplished by cross correlation with a locally generated version of the pseudorandom carrier.*

The two most common forms of spread spectrum, DS/SS and FH/SS, are discussed in the following two subsections.

2.2 Direct Sequence Spread Spectrum (DS/SS)

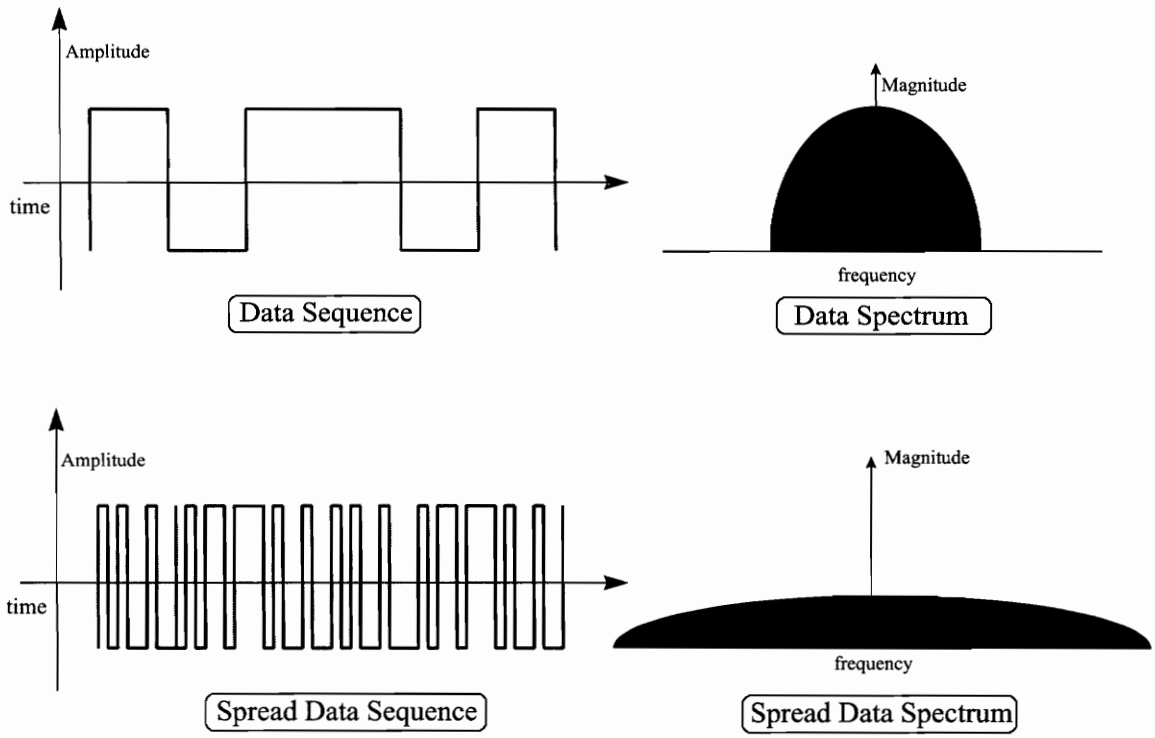

Figure 2.1: Illustration of Direct Sequence Spread Spectrum [19].

In Direct Sequence Spread Spectrum (DS/SS), a user's data stream is modulated by a *spreading code* (i.e., a PN code sequence with low auto correlation properties) which has a rate much higher than the original signal. The symbols of the spreading code are referred to as *chips*. The resultant signal has a bandwidth many times larger than that of the original signal. As an example, if the original signal has a bandwidth of B_u and the spreading code has a bandwidth of B_c then the transmitted signal has an approximate bandwidth $B_{tx} \approx B_u + B_c$ (assuming proper filtering to remove unwanted images). Figure 2.1 shows time and frequency representations of the user data sequence before and after modulation by the spreading code and illustrates that the rise in the signaling rate due to spreading results in an increase in the bandwidth of the user's data signal. The factor N by which

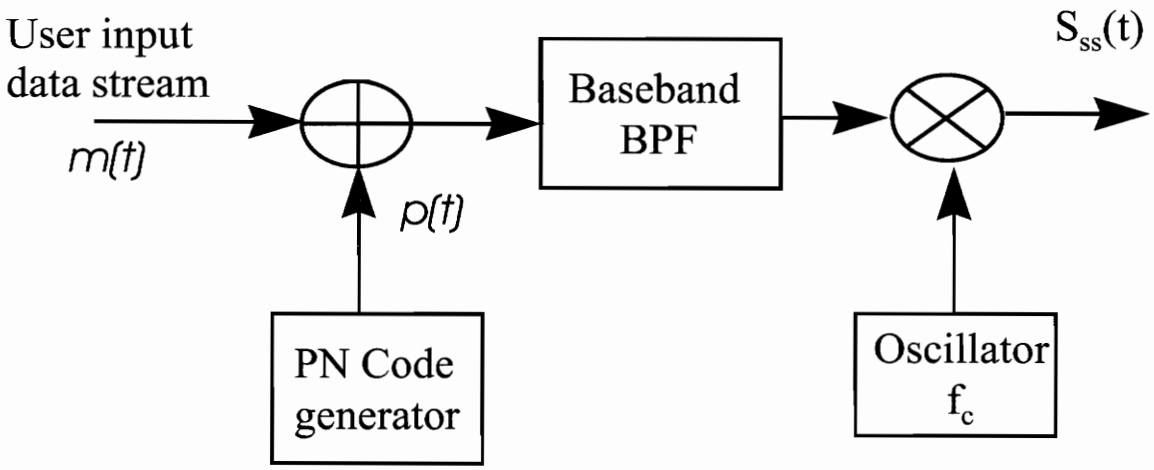

Figure 2.2: Block diagram of a Direct Sequence Spread Spectrum transmitter (binary phase modulation is implied) [25].

the original signal bandwidth is spread is called the *processing gain* or *spreading gain* of the system. Figure 2.2 shows a block diagram of a DS/SS transmitter employing binary phase modulation. The block diagram shows that the user's input symbols are first multiplied (i.e., modulo 2 addition) by the user's spreading sequence and then filtered before being mixed to the carrier frequency f_c. The resultant signal can be represented by

$$s_{DS}(t) = A \cdot m(t) \cdot p(t) \cdot cos(2\pi f_c + \theta) \tag{2.1}$$

where A is the amplitude, $m(t)$ is the user data sequence, $p(t)$ is the PN spreading sequence, and θ is the carrier phase angle at time $t = 0$ [25].

At the receiver, the original data sequence is recovered by correlating the received signal with a locally generated version of the PN spreading sequence used by the transmitting user. A particularly attractive feature of DS/SS is its robustness in the presence of narrowband interference. As an illustration, Figure 2.3 shows a spectral representation of a DS/SS signal received along with narrowband interference before despreading and Figure 2.4 shows the spectrum of the same DS/SS signal after despreading. In the despreading process, the received signal is despread to its original bandwidth while the narrowband interference is effectively spreaded by the factor N. After despreading, filtering can remove most of

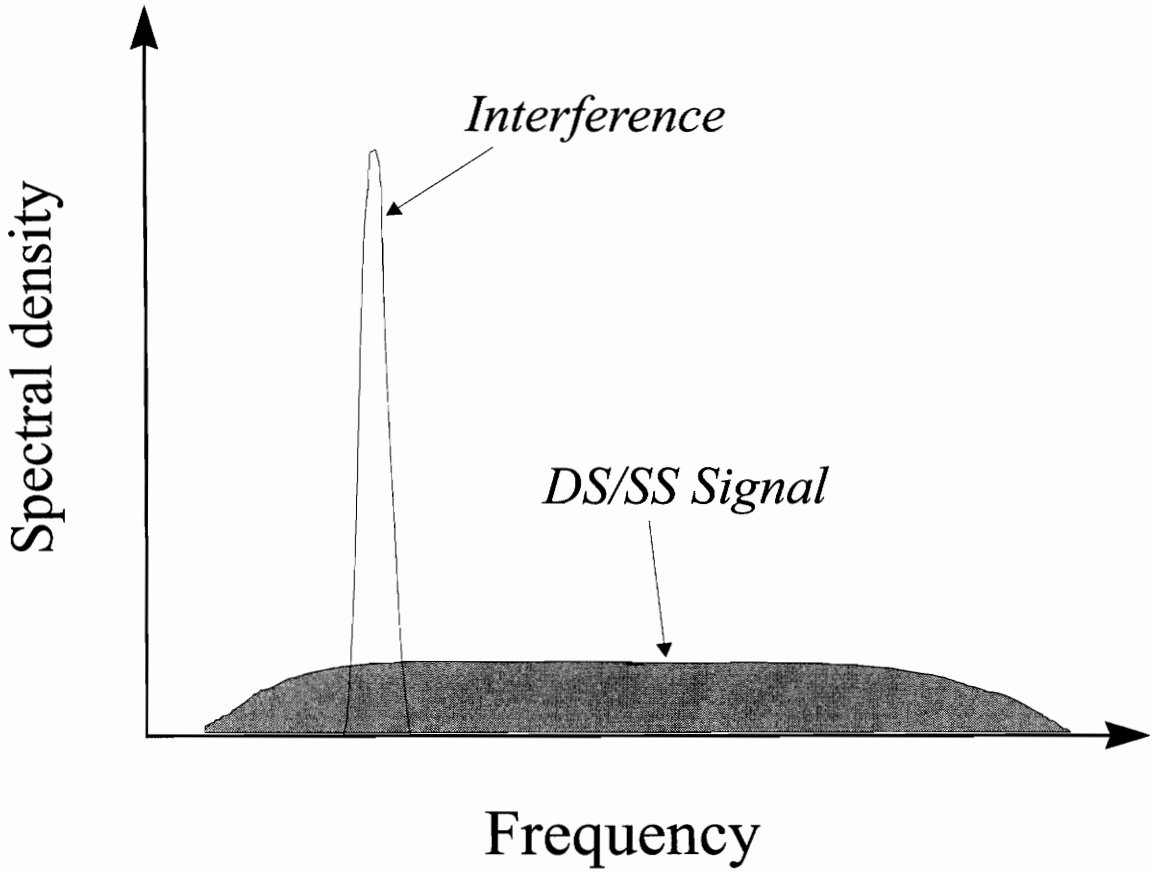

Figure 2.3: Spectrum of desired received DS/SS signal and narrowband interference [25].

the original interference energy. Since only the noise remaining in the band in which the despread signal occupies is retained after filtering, a DS/SS receiver's interference rejection capability is approximately measured by N.

If the active users in a DS/SS system utilize orthogonal spreading codes then their transmissions will have low cross correlation[1] with transmissions of other users in the system and multiple access capability is achieved. Thus orthogonal spreading codes allow multiple users to share a common bandwidth. Utilization of unique spreading codes by users in a DS/SS

[1]Ideally, DS/SS CDMA can provide zero cross correlation between users in the system but this idealistic case cannot be achieved on the mobile to base station link in a realistic network due to imperfect synchronization and multipath effects.

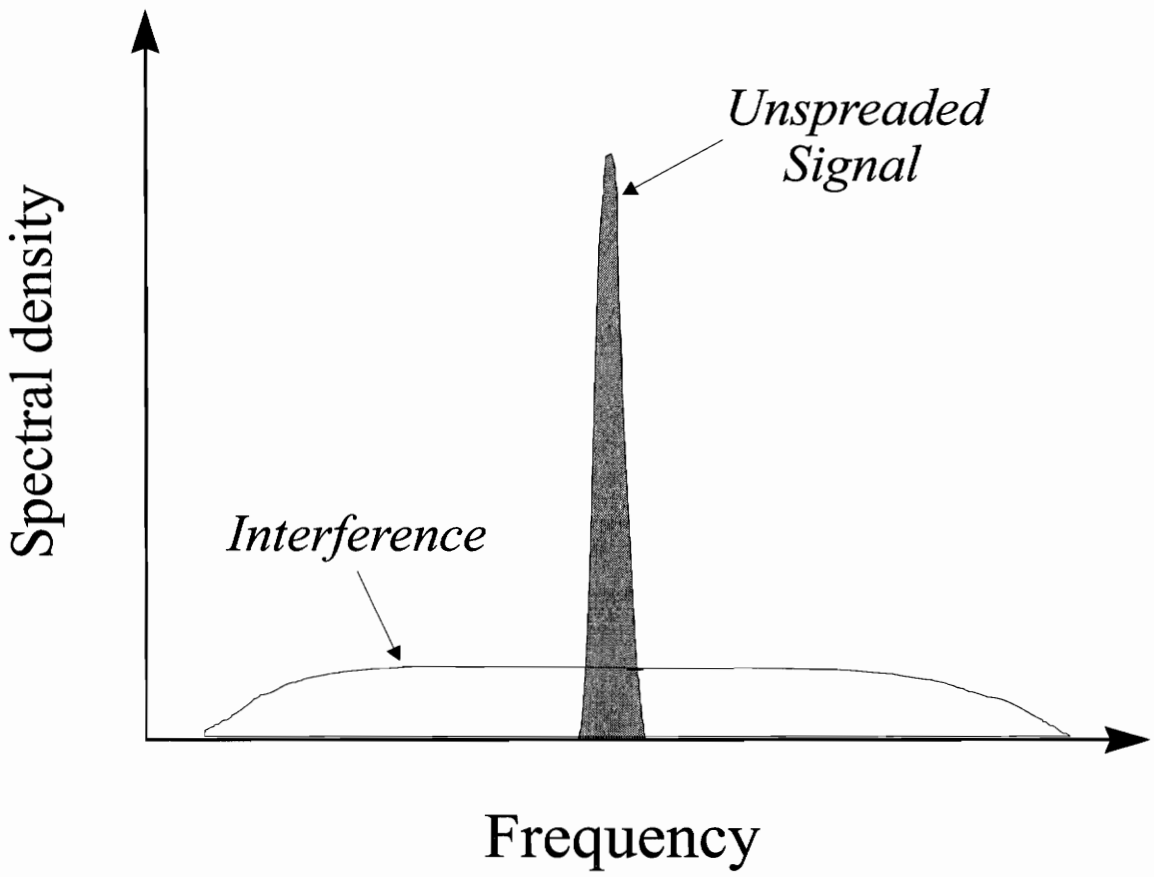

Figure 2.4: Spectrum of desired received signal and interference after despreading [25].

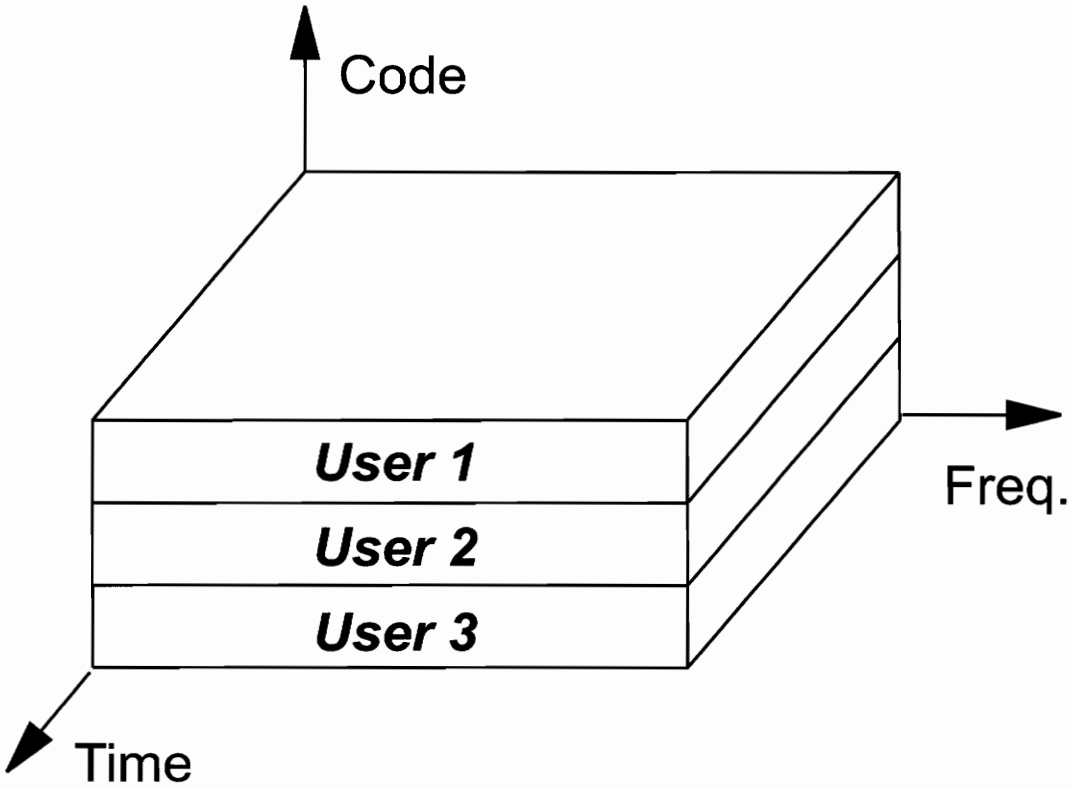

Figure 2.5: Illustration of Code Division Multiple Access (CDMA) in which user channels share the time/frequency space but are assigned unique and orthogonal spreading code sequences [Libe].

system is a form of Code Division Multiple Access (CDMA). Figure 2.5 graphically illustrates that CDMA allows users to share the available time-frequency space while providing multiple access capability through the use of PN spreading codes. In this thesis, we will not consider DS/SS further. Instead we will consider the second major class of spread spectrum, Frequency Hopped Spread Spectrum. For a more complete overview of CDMA or DS/SS we refer the reader to [4], [8], [17], [18], and [19].

2.3 Frequency Hopped Spread Spectrum (FH/SS)

In Frequency Hopped Spread Spectrum, several users can share a common bandwidth by utilizing unique "hopping patterns" to hop their carrier frequencies among a finite set of frequency slots. Utilization of unique hopping patterns by the active users can be considered a form of CDMA although this term has recently become more strongly associated with DS/SS [2]. Systems where the users employ unique hopping patterns to gain multiple access capability to an available bandwidth are termed Frequency Hopped Multiple Access (FHMA) systems.

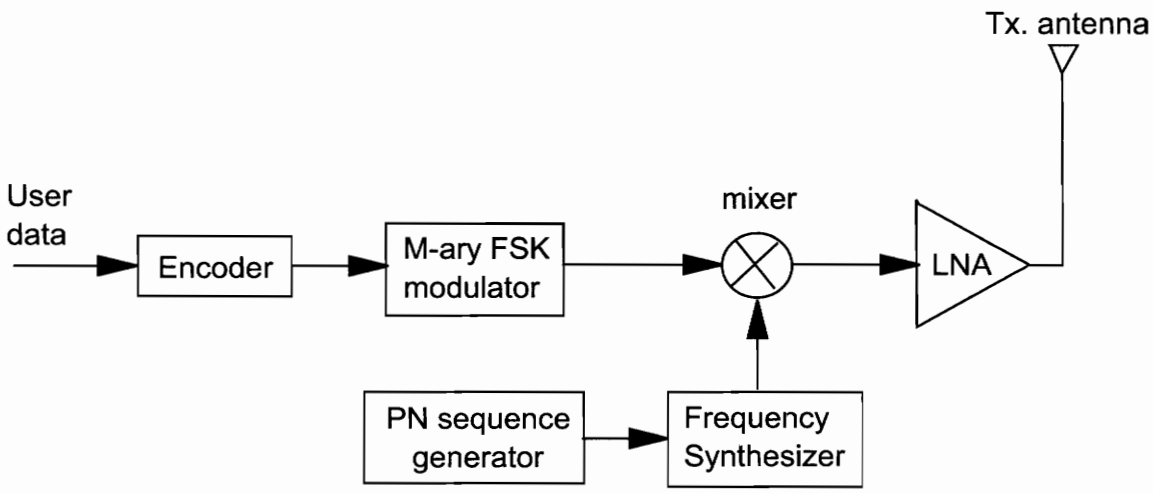

Figure 2.6: Block diagram of a frequency hopping transmitter. [Proakis]

In FHMA systems, the available bandwidth is usually divided into a large number of frequency slots. In most FHMA systems, the frequency slots are contiguous but this is not a requirement. During any signaling interval each active user transmits in one (or possibly more) of the available frequency slots. Figure 2.6 shows the block diagram of a FH/SS transmitter where it is seen that after encoding, the user's data stream undergoes modulation and then periodic frequency translation (by means of the frequency synthesizer)

[2]The strong association of CDMA with DS/SS is no doubt a result of the recent and widespread success of Qualcomm's CDMA cellular, PCS, satellite, and WLL products which use DS/SS

to one of the carrier frequencies corresponding to a frequency slot in the available bandwidth. The modulation is usually either binary or M-ary Frequency Shift Keying (FSK) which allows for noncoherent detection at the receiver. Phase Shift Keying (PSK) modulation (which can provide better performance than FSK modulation under many circumstances) is rarely employed in FH/SS systems due to the difficulty in maintaining phase coherence between hops [18]. The selection of the frequency slot(s) in each signaling interval is made with a pseudo-noise (PN) generator. The signal leaving the FH/SS transmitter can be expressed mathematically as

$$s_{FH}(t) = A \cdot cos(2\pi f_i t + \theta_i) cos(2\pi f_h t + \theta_h) \tag{2.2}$$

where A is the signal amplitude, f_i is the FSK modulation frequency, f_h is the carrier frequency chosen by the frequency synthesizer, and θ_i and θ_h are the phases of the FSK modulator and frequency synthesizer respectively at time t=0.

Reception of the hopped signal at the receiver is accomplished with an identical PN generator which recreates the transmitting user's *hopping sequence*, allowing the receiver to hop synchronously with the transmitter. Figure 2.7 illustrates a situation where there are two active transmitting users (users 'A' and 'B') employing FH/SS in the system . The x-axis represents time and is subdivided into time slots while the y-axis represents the available frequency slots (labeled 1-10)[3]. In Figure 2.7 the active users hop to new frequency slots at the same instants in time. This is termed *synchronous hopping*. In Figure 2.7 it is seen that in time slot 1 user A transmits in frequency slot 10 while user B transmits in frequency slot 1. In the next time slot, user A transmits in frequency slot 7 while user B transmits in frequency slot 3. User A's frequency hopping pattern for time slots 1-7 can be traced to being 10,7,5,8,2,4,6 (i.e., referencing the frequency slot numbers) while user B's frequency hopping pattern for time slots 1-7 can be traced to being 1,3,9,2,7,10,8. If the hopping patterns of users A and B are specifically coordinated so that the users never

[3]This is a simplified example since realistic FHMA systems would typically employ a much larger number of frequency slots

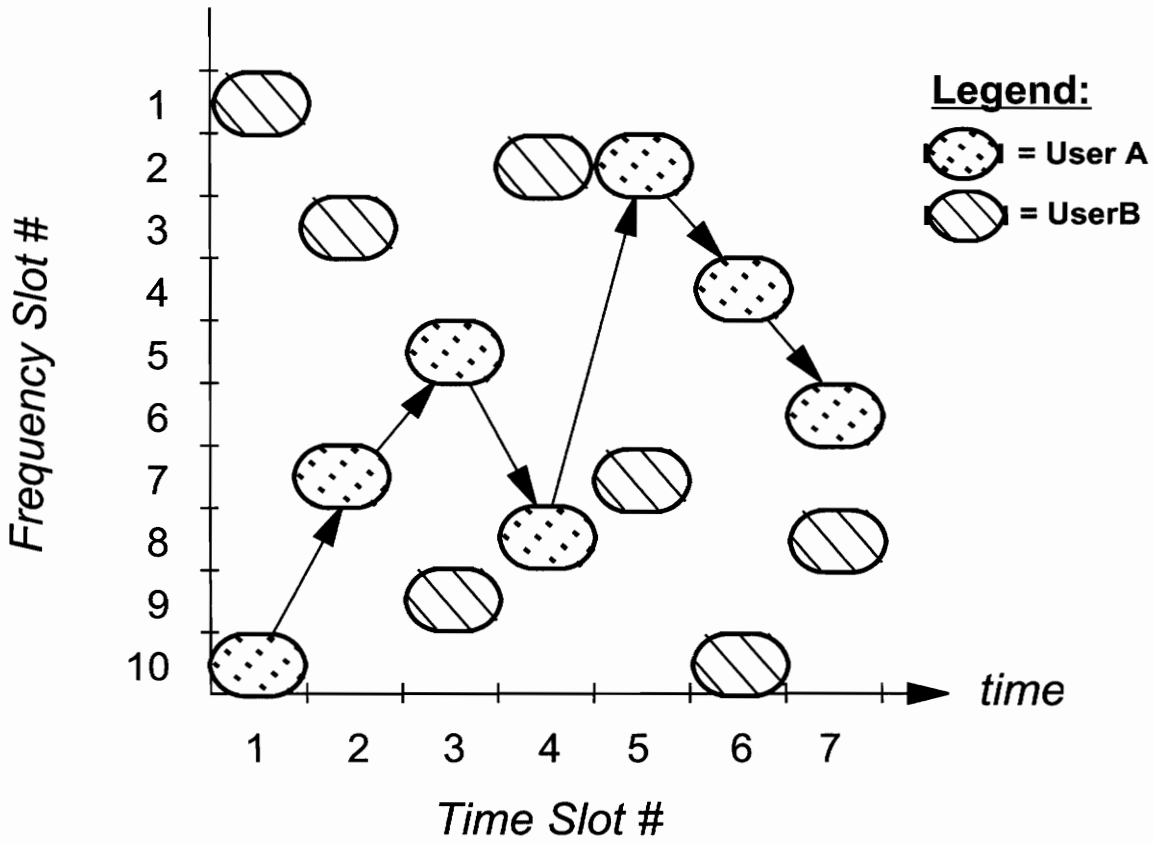

Figure 2.7: Example of frequency hopping with two active users (A and B) hopping among 10 available frequency slots.

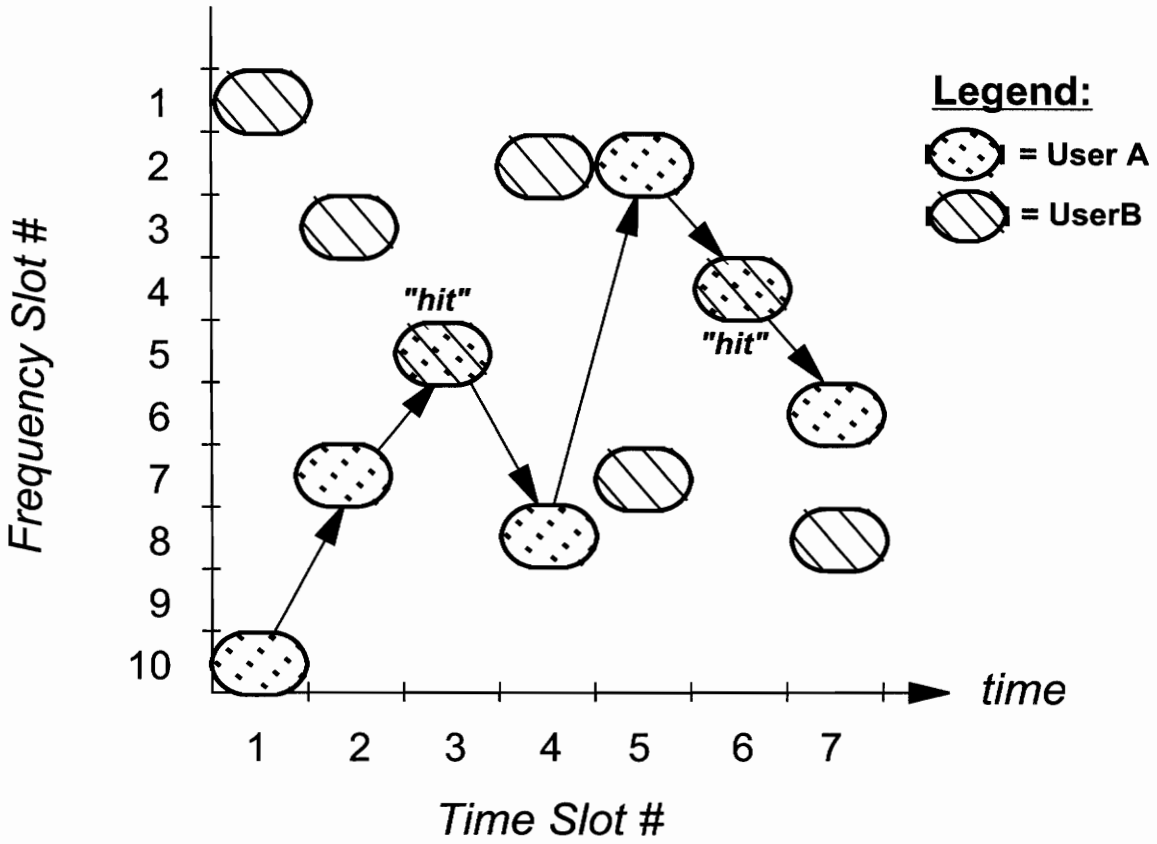

Figure 2.8: Example of frequency hopping with two active users (A and B) employing non-orthogonal hopping patterns.

transmit in the same frequency slot during any given time slot then their hopping patterns are said to be *orthogonal.* If users A and B use *non-orthogonal* hopping patterns then "collisions" or "hits" will occur when the two users transmit in the same frequency slot at the same time. Figure 2.8 illustrates a synchronous hopping system in which users A & B employ non-orthogonal hopping patterns resulting in hits in time slots 3 and 6. Hits often result in corrupted symbols for both users. The idea of orthogonal and non-orthogonal hopping patterns may be extended to any number of users in the system [4].

[4]The number of active users in an orthogonally hopped system is limited by the number of frequency slots in the available bandwidth.

FHMA systems in which the users do not synchronize their hops with other users are termed *asynchronous hopped* systems. Asynchrononous hopped systems are by nature non-orthogonal.

It has been shown by Geraniotis and Pursley in [28] that the probability of a hit in a synchronous non-orthogonally hopped system with m users and q frequency slots is

$$p_{h,m} = 1 - \left(1 - \frac{1}{q}\right)^{m-1} \tag{2.3}$$

and the probability of a hit in an asynchronous non-orthogonally hopped system [5] with m users and q frequency slots is approximated by

$$p_{h,m} \cong 1 - \left(1 - \frac{2}{q}\right)^{m-1}. \tag{2.4}$$

An orthogonal hopping scheme can provide superior throughput performance over a non-orthogonal hopping scheme but cannot be easily implemented in a decentralized network. This is because orthogonal hopping requires careful assignment and synchronization of the hopping patterns for all the active users in the system. Decentralized systems tend to employ asynchronous hopping while highly centralized systems would tend to employ synchronous (and often orthogonal) hopping. Examples of systems which use orthogonal hopping include GSM/DCS1800 systems, CDPD, and Wireless LANs conforming to the IEEE 802.11 standard. Examples of systems that employ non-orthogonal hopping include unlicensed devices, the SINCGARS system, and other military packet radio systems [33].

FHMA can provide several advantages over non-hopped narrowband systems. One advantage is that FHMA provides a form of frequency diversity by exploiting the frequency selective nature of a wide bandwidth. In particular, FHMA can improve the performance in a slow fading environment since the fading process (often a significant source of channel errors for mobiles in narrowband systems) is nearly decorrelated from hop to hop. The fading process is decorrelated because the available bandwidth over which frequency hopping takes place is much larger than the coherence bandwidth. Thus fading experienced

[5] The probability of a hit in an asynchronous system is greater than in a synchronous system because a given interferer may collide with the desired user during two hops instead of only one.

during a particular time interval in one frequency slot may not be experienced at other frequency slots during the same time interval. Therefore there is a significant probability that a hopping user who experiences fading in a frequency slot will hop into a useable (i.e., unfaded) frequency slot during the next time interval. Therefore, FHMA systems can often operate in slow fading environments where non-hopped narrowband systems would experience extended periods of signal loss.

Another advantage of FHMA systems is that they provide interference diversity by averaging the interference generated by all other users in the system. This nearly eliminates the possibility of a single rogue user from either disrupting an entire system or making the system unusable for any particular user in the system. For example, a single user can jam a non-hopped transmission by transmitting an interfering high power signal (thereby lowering the carrier to interference (C/I) ratio for the desired user) in the same bandwidth that communication is taking place between two non-hopped users. In a FHMA network however, the active users will at worst experience the interference caused by a rogue hopping user during a few random time slots. If the interferer is non-hopping, some FHMA systems can even employ techniques to hop around the interferer [31].

A third advantage of FHMA systems is that they provide a high level of security. An eavesdropping user would need perfect knowledge of a user's hopping sequence as well as the ability to hop synchronously with a desired user's transmission in order to intercept it. FHMA's inherent security features has made it popular in military applications for a number of years. Because secure mobile communications is also highly desired in many business applications, commercial FHMA systems have been gaining in popularity [6].

FHMA also provides several benefits over non-hopped DS/SS CDMA systems. One advantage of FHMA over DS/SS CDMA is that FHMA techniques are more resistant to the near/far problem. DS/SS CDMA systems are highly subject to the near/far problem and require accurate power control schemes to obtain the capacity benefits that these systems

[6] An example is Geotek's FHMA voice/data network which is being deployed in major metropolitan cities worldwide.

boast [5]. FHMA's inherent resistance to the near/far problem makes it more practical than DS/SS CDMA for decentralized networks [7] in which tight power control may be difficult to implement.

Another advantage of FHMA over DS/SS CDMA is that discontigous blocks of spectrum may be aggregated to provide the available bandwidth. In contrast, DS/SS CDMA methods require contiguous (and often relatively large) blocks of spectrum for operation. The ability to aggregate several discontiguous blocks of spectrum provides flexibility in spectrum management for FHMA systems as compared to DS/CDMA systems.

A third advantage of FHMA over DS/SS CDMA is that the synchronization requirements for FHMA techniques are typically less stringent than DS/SS CDMA techniques. We refer the reader to [18] for an introduction to synchronization of spread spectrum systems.

This chapter provided an introduction to DS/SS and FH/SS. In the remainder of this thesis, we will focus mainly upon synchronous and asynchronous non-orthogonally hopped FHMA systems. The next chapter introduces error correction coding as the primary means of combating "hits" in FHMA systems.

[7] In many centralized networks, DS/SS CDMA can provide greater total system capacity than FHMA. For an example where the reverse is true, see [34]

Chapter 3

Error Correction Coding

Digital communications over terrestrial wireless channels (e.g., cellular communication) are usually characterized by high error rates compared to communications over wireline mediums (e.g., fiber, twisted pair). For example, error rates on the order of 10^{-10} (i.e., one bit error per ten billion transmitted bits) are typical on fiber optic links whereas error rates on the order of 10^{-3} (i.e., one bit error per thousand transmitted bits) are typical in landline cellular networks. Because Bit Error Rate (BER) or similarly defined block or packet error rates are often the most important parameter from a communication systems user point of view [20], wireless engineers are highly motivated to design systems which provide reliable (i.e., low BER) communication. Theoretical work by Shannon in 1948 and 1949 [21] [22] proved that arbitrarity low error rate communications is possible on a channel (irrespective of whether wireless or landline) provided the information rate D_R (bits/sec) is less than the capacity of the channel C (bits/sec). Shannon's results have provided theoretical performance bounds which designers of practical systems can strive to achieve. Systems which approach Shannon's bound must use error correction coding [23] to achieve their high level of performance.

Error correction coding (or channel coding) is a powerful technique for improving (i.e., lowering) BERs in practical systems. Bit errors in wireless communication systems are typically attributed to ambient noise, interference, or multipath fading effects which can cause the received signal power to fall below the noise floor. It is well known that BER performance at the receiver can often be improved by increasing the transmission power at the transmitter. However, this is usually an impractical solution for mobile applications where the transceiver is small (i.e., cellular/PCS, wireless LANs, etc.) and transmitter power is

limited [1]. Furthermore, in multi-cell cellular systems, increasing transmitter power simply increases the co-channel interference in the system thereby not always resulting in improved performance. Therefore, most wireless systems employ a form of error correction coding which can help achieve low BER performance at reduced transmitter power levels [20]. The function of an error correction code is to introduce some redundancy to the transmitted data sequence which can be used at the receiver to detect and/or correct bit errors caused by the channel. The capability to detect/correct errors at the receiver offers a powerful technique for mitigating the effects of noise, interference, or fading encountered in the transmission of the signal through the wireless channel. The amount of redundancy introduced by encoding the data is measured by the code rate $R = k/n$ which is the ratio of the number of information symbols transmitted per code word k to the total number of symbols transmitted per code word n. The amount of BER improvement that a error correction code provides is usually quantified by the *coding gain*. The coding gain is the amount of additional transmitter power which would be required to provide equal performance without the error correction code. The two most popular classes of channel codes used in modern wireless communications systems are convolutional codes and block codes. Both types are briefly discussed in the following subsections.

[1] In fact, one advantage of DS/SS CDMA which contributes to its commercial success is the reduced transmit power requirements afforded by this technology. Reduced transmit power translates directly into extended talk time for CDMA PCS phones, a highly desired feature in the commercial arena.

3.1 Convolutional Codes

Convolutional encoders convert a user's entire data stream into one long code word. The user's data stream is read in blocks of k input bits which produce blocks of n output bits (where $n > k$). In convolutional coding schemes, the values of k and n are usually small and the output bits depend on the current input bits as well as the state of the convolutional encoder. Figure 3.1 shows an example of a rate 1/2 convolutional encoder where k=1 and n=2. The example rate 1/2 encoder has a single shift register with 2 stages (In general, a convolutional encoder contains one shift register for each input.). A convolutional encoder is defined by the number of stages in the shift register(s), the number of outputs, and the connections between the shift register(s) and the modulo-2 adders [24]. The contents of the shift register are completely determined by the initial state of the shift register (usually all 0's) and the previous information bits already fed into the shift register. Any convolutional encoder can be fully described by its set of generator polynomials; one generator polynomial for each output/input combination. Alternative methods for describing convolutional encoders include tree diagrams, trellis diagrams, and state diagrams. We refer the reader to [18] for a general overview of these representations. The generator polynomials for the example encoder of Figure 3.1 are

$$g_1 = [111] \tag{3.1}$$

$$g_2 = [101]. \tag{3.2}$$

A '1' in the ith position of a generator polynomial vector indicates that the corresponding stage in the shift register is connected to the modulo-2 adder of the given output [18]. A '0' in the ith position of a generator polynomial vector indicates no connection exists between the corresponding stage in the shift register and the modulo-2 adder for the given output. Thus $g_2 = [101]$ indicates that the user data stream and second stage of the input shift register are connected to the modulo-2 adder of the second output $y2$. The number of stages in the longest shift register (i.e., if there are multiple shift registers) of the convolutional encoder determines the constraint length K. K is the maximum number of bits in a single output

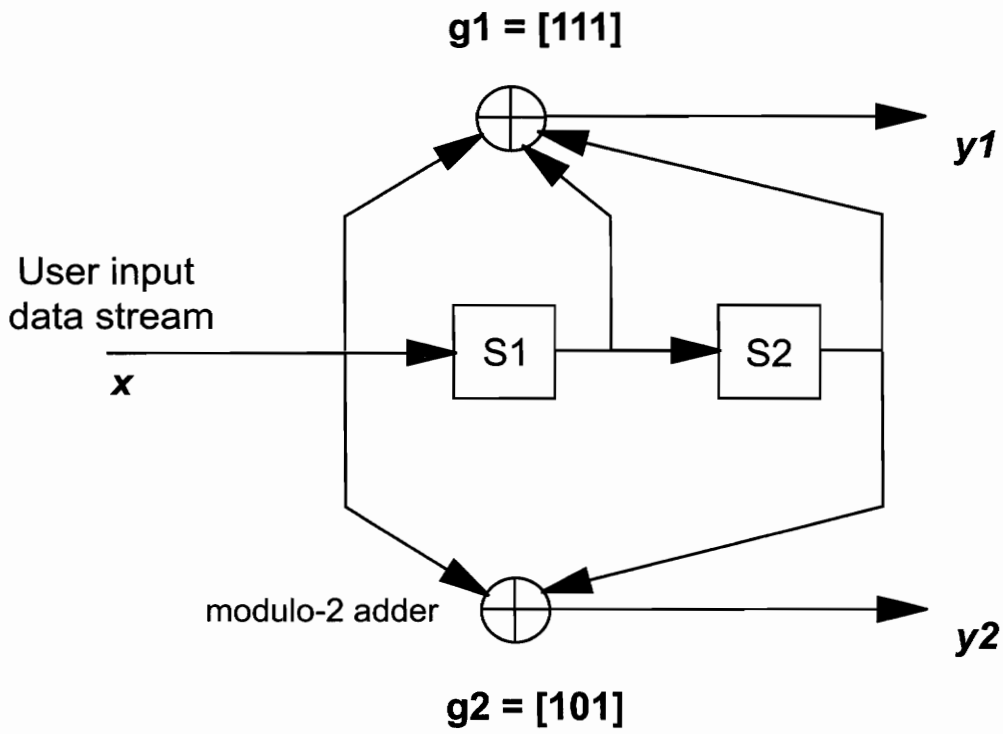

Figure 3.1: Example of a typical rate 1/2, constraint length 3 convolutional encoder.

stream that can be affected by any input bit and is equal to the length of the longest input shift register plus one. In the example encoder of Figure 3.1, K=3 since the shift register has 2 stages.

Optimum decoding of a convolutional code is usually accomplished with the Viterbi algorithm which is a maximum likelihood sequence estimation (MLSE) algorithm [29]. The Viterbi algorithm takes as its input the received encoded sequence (possible corrupted by the channel) and decodes the received data by determining the most probable transmitted sequence according to the trellis of the code. Viterbi decoding is the most popular algorithm for decoding convolutional codes of short constraint lengths (i.e., $K \leq 10$) while another algorithm, Sequential decoding, is popular for long constraint length codes.

The *minimum free distance* d_{free} of a convolutional code generally determines the error rate performance of a the code. d_{free} (or equivalently, the error rate capability of the code)

can be increased by either decreasing the code rate R or by increasing the constraint length K of the code. The probability of decoder error for a hard-decision Viterbi decoder is upper bounded by

$$P_{de} < \sum_{d=d_{free}}^{\infty} a_d \left[4p(1-p)\right]^{d/2}, \tag{3.3}$$

where the coefficients a_d represent the number of paths in the code's trellis corresponding to the set of distances d, and p is the probability of a bit error in a binary symmetric channel.

Convolutional codes have been a popular choice in cellular and PCS systems because they introduce less latency in the transmitted data than do many alternative coding schemes such as long block codes [2]. Although long block codes often have more powerful error correction capabilities (for similar rate codes), the low latency imposed by convolutional decoders is critical in cellular and PCS systems where the majority of traffic is real-time voice rather than data. In addition, convolutional encoding/decoding chipsets are relatively cheap and available from a number of ASIC manufacturers including Qualcomm. Examples of commercial application of convolutional coding include the IS-95 CDMA Cellular/PCS standard, the IS-54/136 [3] standard, and the GSM/DCS-1800 [4] standard. The IS-54/IS-136 standards employ R=1/2, K=6 convolutional codes and the GSM/DCS-1800 standards specify R=1/2, K=5 convolutional coding. The IS-95 standard specifies a R=1/2, K=9 convolutional code on the forward link (i.e., base station to mobile) and a R=1/3, K=9 convolutional code on the reverse link (i.e., mobile to base station) [25]. The reverse links employ a lower code rate because they require more powerful error correction to combat higher interference levels due to the non-orthogonal CDMA transmissions of the mobile users.

[2] Although short block codes may not introduce unacceptable latency to applications, they often underperform convolutional codes. Block code performance generally increases with block length. Thus, although many long block codes can often outperform convolutional codes (at the expense of increased latency), shorter block codes may actually underperform convolutional codes.

[3] IS-136 is essentially identical to IS-54 but is designed for operation in the PCS band.

[4] DCS-1800 is essentially identical to GSM except that the operating frequencies correspond to the PCS band rather than the 800-900 MHz cellular frequencies

3.2 Block Codes

A block code generally takes k user information symbols and maps each k symbol block into a larger n symbol code word. The number of parity check symbols is equal to $n-k$ and the code rate R of the block code is equal to k/n. Figure 3.2 illustrates the concept of a binary block encoder (i.e., it is a "binary" encoder since the information and code symbol elements are chosen from a binary alphabet of either '0' or '1'). In Figure 3.2 a k=4 bit block of user data enters the binary encoder producing an n=7 bit code word at the output of the encoder. In this example, the resultant code word is equivalent to the k bit user input block plus $n-k$=3 parity check bits (labeled p1, p2, & p3). Block encoders which arrange the information bits at the beginning of the code word followed by the parity check bits are called *systematic* encoders. The particular values of the parity check bits depends on the design of the encoder and the k bit input block. The parity check bits provide error detection and/or error correction capability because they are functionally related to the k bit information block by modulo-2 arithmetic. A block encoder can be fully described by its generator matrix G which is a $k \times n$ (i.e., k rows by n columns) matrix that includes a $k \times k$ identity matrix followed by a $k \times (n-k)$ matrix Z which determines the set of code words (or equivalently parity check vectors) which user input data blocks may be mapped to. An example of a generator matrix for the (7,4) encoder of Figure 3.2 could be

$$G = \left[I_{k\times k} | Z_{k\times(n-k)} \right] \tag{3.4}$$

$$= \begin{bmatrix} 1 & 0 & 0 & 0 & | & 0 & 1 & 1 \\ 0 & 1 & 0 & 0 & | & 1 & 0 & 1 \\ 0 & 0 & 1 & 0 & | & 1 & 1 & 0 \\ 0 & 0 & 0 & 1 & | & 1 & 1 & 1 \end{bmatrix}. \tag{3.5}$$

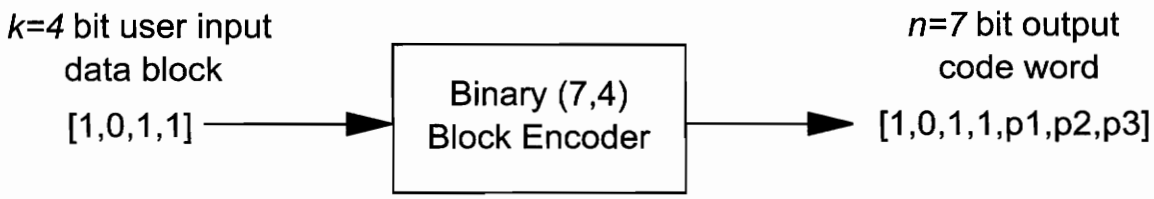

Figure 3.2: Illustration of a (n=7,k=4) binary block encoder.

In this case, the 4 bit user input block of [1011] would result in the code word

$$c = m \times G = \begin{bmatrix} 1 & 0 & 1 & 1 \end{bmatrix} \cdot \begin{bmatrix} 1 & 0 & 0 & 0 & | & 0 & 1 & 1 \\ 0 & 1 & 0 & 0 & | & 1 & 0 & 1 \\ 0 & 0 & 1 & 0 & | & 1 & 1 & 0 \\ 0 & 0 & 0 & 1 & | & 1 & 1 & 1 \end{bmatrix} = \begin{bmatrix} 1 & 0 & 1 & 1 & 0 & 1 & 0 \end{bmatrix}. \tag{3.6}$$

Therefore, with the generator matrix defined by (3.5) the encoder produces the 7 bit code word [1011010] consisting of the original 4 bit information sequence [1011] appended with the parity check bits [010].

The weight of a code word or error pattern is the number of nonzero coordinates in the code word or error pattern [20]. For example, if the transmitted code word is s_{tx}=[10111] and the received word is s_{rx}=[10100] then s_{tx} has a weight of 4, s_{rx} has a weight of 2, and the error pattern (i.e., e=[00011]) has a weight of 2.

The number of available code words is limited by the number of possible unique k bit input message sequences which may enter the encoder. For example, in the case of the (7,4) binary encoder of Figure 3.2 there are $2^k = 2^4 = 16$ unique 7 bit code words corresponding to the 16 possible unique k=4 bit input messages.

The *Hamming distance* between two blocks w and x is the number of coordinates in which the two blocks differ. For example, if w=[10111] and x=[10100] then the Hamming distance between w and x is 2 since the two blocks differ in exactly two coordinates (specifically the 4th and 5th coordinates). The *minimum distance*, d_{min}, of a block code is the minimum Hamming distance between all distinct pairs of code words in the code. The

minimum distance determines the detection/correction capabilities of the block code. In general, a block code with minimum distance d_{min} can detect all error patterns of weight less than or equal to $(d_{min} - 1)$ [20] or correct all error patterns of weight less than or equal to $\lfloor (d_{min} - 1) \rfloor /2$.

Block codes are very popular in data communication systems where minimizing latency is not as critical as in real-time voice communications. Arguably the most powerful in the family of block codes are the Bose-Chaudhuri-Hocquenghem (BCH) and Reed-Solomon (RS) codes [20]. One advantageous feature of BCH and RS codes is that they provide a designer a large selection of block lengths and code rates. The RS codes (sometimes thought of as non-binary BCH codes) are especially powerful codes with optimal distance properties (and therefore optimal error detection/correction properties). The next subsection provides an overview of RS codes and their error detection/correction properties.

3.2.1 Reed-Solomon Block Codes

Reed-Solomon (RS) codes are a special class of non-binary BCH codes which have become popular in cellular, satellite, and deep space communication systems as well as in optical data storage systems. An (N,K) RS code has a block length of N non-binary symbols. A number K of these non-binary symbols are information symbols and the remaining $N-K$ symbols are parity check digits. Each non-binary symbol in the RS code is usually chosen from an alphabet of $q = 2^x$ elements (where x is a positive integer). When the alphabet size is a power of 2, each q-ary element has an equivalent binary representation consisting of x bits. Thus, a RS code with a block length of N can be mapped into a binary code of block length $n = x \cdot N$. As an alternative to transmitting x bits per q-ary symbol, a single M-ary FSK waveform (where $M = q$) may be transmitted per code symbol. Figure 3.3 illustrates the function of a systematic (N=7,K=4) RS encoder where the alphabet size is q=8 and each symbol is represented in octal notation. Similar to the binary block encoder of Figure 3.2, the RS encoder of Figure 3.3 appends $N-K$=3 parity check symbols (denoted P1, P2, & P3) to the K=4 symbol user input data block to form the N=7 symbol RS code word.

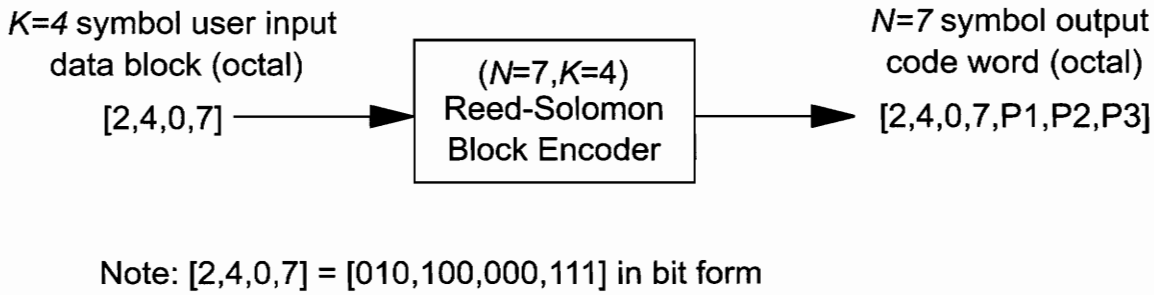

Figure 3.3: Illustration of a (N=7,K=4) Reed-Solomon block encoder.

RS codes are termed Maximum Distance Separable (MDS) codes because they achieve the largest possible minimum distance d_{min} [5] of any linear code with the same encoder input

[5] d_{min} of a block code is analagous to *minimum free distance* d_{free} of a convolutional code.

Table 3.1: Practical block lengths for Reed-Solomon codes

RS block length in symbols (N)	Alphabet size (q)	# bits/symbol (x)
7	8	3
15	16	4
31	32	5
63	64	6
127	128	7
255	256	8

and output lengths [6]. Thus, RS codes provide optimal error detection/correction capabilities when compared to other types of block codes with equivalent length and alphabet size. A (N,K) RS code can correct up to $d = N - K$ symbol erasures or $t = \lfloor (N-K)/2 \rfloor$ symbol errors where $\lfloor \cdot \rfloor$ is the greatest integer operator. Therefore, RS codes (regardless of block length N) can correct approximately twice as many symbol erasures as symbol errors.

Table 3.1 shows the alphabet sizes and number of bits per code symbol for practical length RS block codes.

Although other types of codes may provide slightly better performance in random noise environments, RS codes perform particularly well in channels with bursty error characteristics. This is a particularly good property for terrestrial wireless channels which are characterized by bursty error patterns due to the multipath fading environment typically encountered in such channels [7].

Figure 3.4 illustrates why RS codes can perform particularly well against burst error patterns. In Figure 3.4 the octal sequence [2,4,0,7,5,1,2] (or equivalently, [010, 100, 000, 111, 101, 001, 010] in bit representation) corresponding to an RS code word of block length N=7 is transmitted over a random error channel and a bursty error channel. In both channels, exactly three bit errors occur in transmission of the code word. In the random error channel

[6] Binary MDS codes do not exist except for the trivial repetition type codes.

[7] Another popular application for RS codes is in digital media storage where error patterns tend to be bursty due to occasional defects in the magnetic or optical storage media.

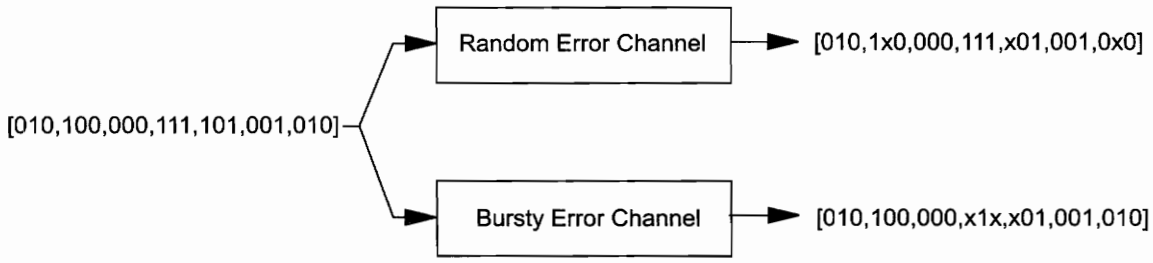

Figure 3.4: Illustration of random and bursty error channels.

case however, the three bit errors result in 3 code symbol errors while the three bit errors in the bursty error channel case result in two symbol errors. Therefore, the RS code would need the capability to correct at least 3 errors in the random error channel case (implying a (7,1) RS code)) but only 2 errors (implying at least a (7,3) RS code) in the bursty error channel case [8]. In other words, since any multiple number of bit errors can be corrected in a corrupted symbol as easily as a single bit error in the same symbol, RS codes are inherently well structured to withstand burst error patterns.

RS codes are very popular in many data communications systems due to their excellent distance properties and burst error correction capabilities. They are not as popular in real-time voice communications as they are in data communications due to the relatively large amount of latency involved in decoding long RS code blocks (see Table 3.1 for RS code block lengths). Another reason for the popularity of RS codes is the existence of efficient hard decision decoding algorithms such as the Berlekamp-Massey algorithm [18] [38] [39]. Efficient algorithms allow practical implementation of relatively long codes. This is an advantage since block code performance improves with increasing block length (as well as with increasing distance properties).

[8] We do not mean to suggest that the absolute number of errors encountered in random error environments is equal to the absolute number of errors encountered in bursty error environments. Usually, bursty error environments (such as multipath fading envionments) have much higher bit error rates than random error environments (i.e., white noise environments).

The probability of decoder error for a hard-decision RS decoder is bounded by

$$P_{de} = \sum_{j=t+1}^{N} \binom{n}{j} p_{se}(m)^j \cdot (1 - p_{se}(m))^{n-j}, \tag{3.7}$$

where t is the number of errors that the (N,K) RS code can correct and p_{se} is the probability of a symbol error (assuming M-ary symbols) [18].

An example of a commercial application of RS coding is the Cellular Digital Packet Data (CDPD) standard which provides a protocol for improved mobile data capabilities to installed analog cellular systems. The CDPD standard specifies a (63,47) Reed-Solomon code which is capable of correcting up to 8 symbol errors (6 bits/symbol) per 378 bit code block.

In this chapter we provided an overview of error correction coding. The most popular classes of codes (i.e., convolutional codes and block codes) were introduced as well as key coding theory concepts such as *minimum distance* and *code rate*. In the next chapter, we introduce the concept of Variable Rate Coding (VRC) and explain how VRC can offer throughput improvements in wireless FHMA data networks.

Chapter 4

Variable Rate Coding

In recent years, wireless service providers have been in a continual search to increase the capacity of their networks. This search has been largely fueled by unrelenting and increasing demand for wireless voice and data services. There are a number of known methods for increasing the capacity of multi-cell wireless networks. Some methods commonly considered include the following:

1: *Increasing the available bandwidth*

2: *Sectoring*

3: *Cell splitting*

4: *Smart antennas*

5: *Interference cancellation techniques*

The first method, increasing the available bandwidth, is probably the easiest way to increase system capacity. Unfortunately, this approach is often impractical due to either the unavailability or prohibitive price of additional bandwidth.

The second method, sectoring, involves using multiple directional antennas in a cell instead of a single omnidirectional antenna. Figure 4.1 illustrates 120 degree sectoring where it is implied that three directional antennas are used in the cell rather than a single omnidirectional antenna. Sectoring increases system capacity by decreasing the co-channel interference experienced at the base stations. Disadvantages of sectoring include increased cost (due to the extra antennas and increased complexity of the base stations), increased

number of handoffs [1], and decreased trunking efficiency. Also, sectoring is often ineffective in dense uban areas where it is difficult to control where the RF energy propagates [25].

The third method, cell splitting, is commonly used in multi-cell systems and is a rather straight forward method of increasing capacity. Cell splitting involves subdividing a congested cell into two or more smaller cells; each with its own base station. The base stations in the new smaller cells usually are designed with reduced antenna heights and transmit power. Cell splitting provides greater system capacity by providing greater reuse of the available bandwidth. Disadvantages of cell splitting include greater system complexity (due to the larger number of cells) and a greater number of handoffs (due to the smaller cell sizes).

The fourth method, employing smart antennas, involves adaptively shaping the base station receive antenna gain pattern [10] [36] [37] to emphasize the signals of desired users as well as null out the signals of interfering users. Thus, smart antennas attempt to increase system capacity by decreasing the co-channel interference experienced at the front end of the base station. Smart antenna technology may become particularly attractive in dense urban environments where severe multipath results in poor C/I ratios (and thus poor performance). A drawback of smart antenna technology is that it is still in development stages and thus is not readily available for commercial deployment. A potential disadvantage of smart antenna technology (at least for a number of years) could be the high additional cost that these systems will add to existing base stations when the technology first becomes readily available [2].

The fifth method, use of interference cancellation techniques, involves adaptively cancelling interfering signals received at the base station thereby improving C/I. As in some of the previously mentioned methods, improvement in C/I translates to greater system ca-

[1] In some modern sectorized base stations, mobiles may be handed off between sectors of the same cell without intervention from the Mobile Switching Center (MSC) thus making the handoff problem of reduced concern [25].

[2] It is possible however that the additional cost per base station (which could initally be as high as $150k-250$k per base station) could still be a better option than cell splitting which would require installing several new base stations

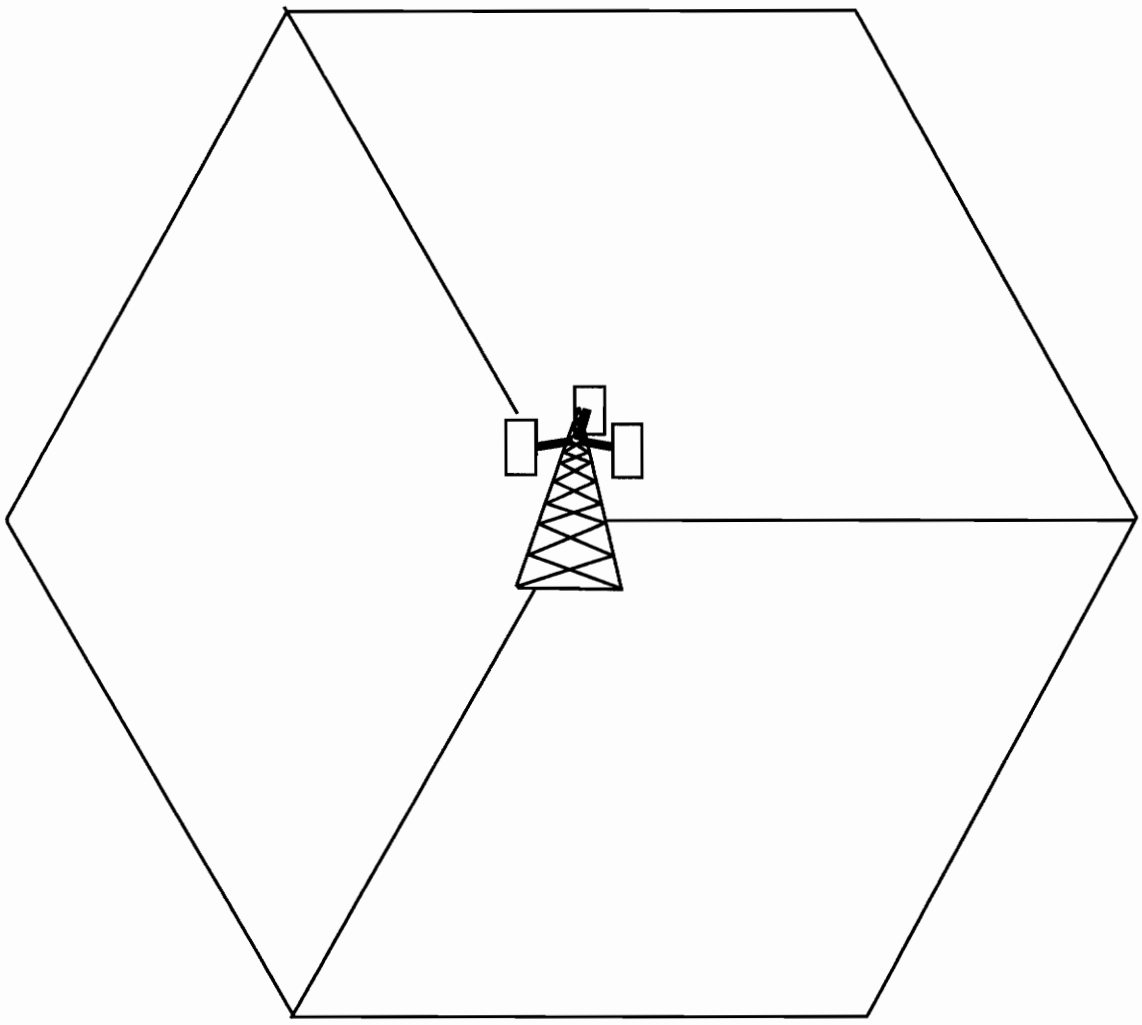

Figure 4.1: Illustration of a base station employing 120 degree sectoring in a cell.

pacity since more users may be allowed in the system. Interference cancellation techniques may take various forms depending upon the particular type of system considered (e.g., Analog, TDMA, or CDMA) and the particular type of signal to be cancelled (e.g., narrowband/wideband). Interference cancellation is currently an important topic of research and will likely be initially deployed at base stations in multi-cell systems in coming years. It is likely that simpler forms of interference cancellation techniques will also be implemented in mobile handsets in the near future.

All five methods mentioned above can be used to achieve greater capacity in wireless networks. The first method achieves its goal by increasing the amount of natural resources (i.e., bandwidth) available to the system while the second through fifth methods attain capacity improvements by mitigating the effects of interference at the receiver.

This thesis proposes an entirely different technique for increasing capacity of wireless networks called Variable Rate Coding (VRC). With VRC, an adaptable code rate is employed during communication allowing a transmitter-receiver pair to adapt the amount of redundancy provided by a code to the quality of the channel. This is opposed to a Fixed Rate Coding (FRC) scheme in which a fixed code rate is utilized to provide sufficient protection for the worst case channel conditions. Practical FRC schemes are inherently inefficient because they are overdesigned for average channel conditions. If estimates of the channel quality are available at the receiver, then VRC can be used to attempt to employ an optimal code rate (i.e., a code rate that provides maximum information throughput) during communication. Therefore, VRC seeks to provide capacity gains in wireless networks by improving the coding efficiency of these systems rather than by reducing the amount of interference seen by the receivers in the system.

VRC techniques are not currently employed in practical systems. One reason is that FRC schemes are much less complicated to design. Another reason is that a VRC scheme is currently impractical for systems where users require small, cheap transceivers such as cellular or PCS systems. This impracticality is a result of the fact that multiple encoder/decoder chipsets would be required in a transceiver to support multiple code rates for the VRC

scheme. Multiple encoder/decoder chip sets are undesirable since such an implementation would result in a large and expensive transceiver. Technological advances in Digital Signal Processors (DSPs) however, could make VRC a practical option in future transceiver design. DSPs could hypothetically allow a transceiver's encoder or decoder to be reconfigured quickly and easily during communication without excessive hardware redundancy.

It is possible that VRC could be implemented in future wireless networks to complement promising interference mitigation technologies such as smart antennas and interference cancellation techniques to achieve much higher capacity systems than exist today. Figure 4.2 illustrates that the capacity benefits offered by VRC are orthogonal to those offered by interference mitigation technologies. In Figure 4.2 distance from the origin represents total network capacity while point 'A' represents the capacity of a present day system. Point 'B' represents the improvement in capacity over a present day system by employing technologies which seek to improve C/I performance (e.g., smart antennas or interference cancellation techniques). Point 'C' represents the improvement in capacity offered by VRC over a system employing FRC and point 'D' represents the capacity of a system employing both VRC and interference mitigation technologies together. The point of this diagram is not to suggest the magnitude of capacity gains that either VRC or interference mitigation technologies can provide relative to present day systems (since such gains would be highly dependent upon the channel characteristics as well as particular implementations of the technologies) but rather that the improvements in coding effieciency that a VRC scheme can provide can complement technologies which seek to improve capacity by improving C/I.

In contrast, capacity gains offered by technologies such as smart antenna systems and interference cancellation techniques are not orthogonal since these techniques attempt to achieve capacity gains in similar ways. Thus if both technologies are perfected, there could be marginal benefit in using the two technologies together in a receiver as opposed to just one[3].

[3]We realize that this is a general statement that could be disproven if it is seen that the two technologies could complement each other under special propagation environments. Both technologies have yet to be

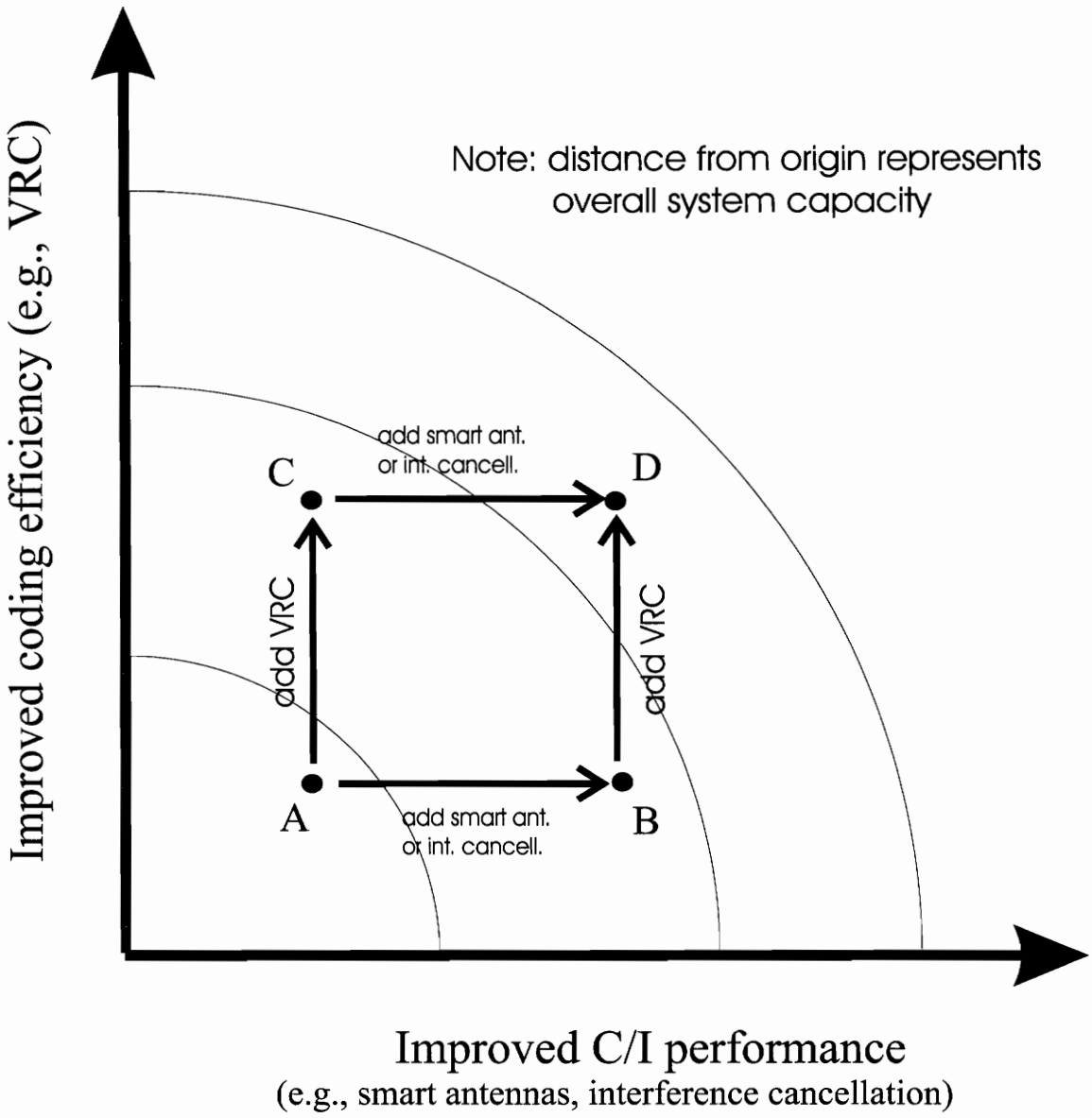

Figure 4.2: Capacity gains provided by variable rate coding (VRC) can augment gains provided by interference mitigation technologies.

It is the purpose of this thesis to determine the magnitude of the capacity gains that a VRC scheme can provide to a FHMA wireless network. In particular, we analyze decentralized FHMA networks in which the users employ non-orthogonal hopping patterns to gain multiple access capability to the available bandwidth. Capacity of a FHMA network can be measured by system throughput. We define the system throughput with m simultaneously transmitting users $W(m) = m \cdot P_c(m)$ to be a measure of the total information flow in the system where $P_c(m)$ is the probability of receiving the correct code word given m transmitting users in the system. In order to form a basis to compare our FHMA system with other multiple-access systems we define normalized throughput given m users $S(m)$ to be the data throughput $W(m)$, normalized by the code rate R and number of frequency slots q, given by

$$S(m) = R \cdot W(m)/q = R \cdot m \cdot P_c(m)/q. \tag{4.1}$$

The number of users m is typically considered to be a random variable which is Poisson distributed with an average value λ [4]. The Poisson distribution is given by

$$p_M(m) = \frac{e^{-\lambda} \cdot \lambda^m}{m!}. \tag{4.2}$$

Figure 4.3 illustrates some throughput curves for an asynchronous hopped FHMA system employing Reed-Solomon coding with block length n=127. The curves in Figure 4.3 were generated by defining the probability of correct reception given m simultaneous users, $P_c(m)$, as

$$P_c(m) = \sum_{j=0}^{n-k} \binom{n}{j} p_{h,m}(m)^j \cdot (1 - p_{h,m}(m))^{n-j}, \tag{4.3}$$

where $p_{h,m}$ is the probability of a hit given m users approximated by

$$p_{h,m} \cong 1 - \left(1 - \frac{2}{q}\right)^{m-1} \tag{4.4}$$

tested in full scale networks to determine their relative or collective practical gains.

[4] i.e. $\lambda = E[M]$ where M is a random variable representing the number of users in the system at a given time

for an asynchronous hopped system [28].

The final throughput expression given m users for the asynchronous hopped FHMA system employing RS n=127 coding is

$$S(m) = \frac{m}{q}\sum_{j=0}^{n-k} R \cdot \binom{n}{j}\left(1-\left(1-\frac{2}{q}\right)^{m-1}\right)^{j} \cdot \left(1-\left(1-\left(1-\frac{2}{q}\right)^{m-1}\right)\right)^{n-j}. \quad (4.5)$$

It is assumed that the receivers have no side information (i.e., no information on when "hits" occur) and thus rely on the RS code's error correction capabilities to mitigate the effects of multiple access interference (MAI) [5]. Throughput curves for m=2, 4, 6, & 8 users are shown plotted as a function of the code rate R. In each case, it is observed that for each m there is an optimal code rate R_{opt} which corresponds to a peak achievable throughput. For the case of $m = 2$ users, the optimal code rate is $R_{opt} = 0.92$ which corresponds to a peak throughput of 0.0148. Similarly, for the case of $m = 4$ users, the optimal code rate is $R_{opt} = 0.83$ which corresponds to a peak throughput of 0.0259. If estimates of m are available, then it is possible to implement a VRC scheme which could attempt to always employ the optimal code rate R_{opt} corresponding to the peak throughput achievable given the MAI in the system [6].

Estimates of m might possibly be made by monitoring the activity levels in a fixed number of frequency slots and relating the measured activity to m. Alternatively, a blind estimation algorithm may be used where upon commencement of communication, the transmitter incrementally increases the transmission code rate from some nominal rate until the receiver measures that increasing throughput no longer occurs. From this information, it is possible to identify approximately where the throughput peak (and thus the optimal code rate $R_{var}(m)$) occurs. However, it is not the purpose of this thesis to explore these or other methods of obtaining accurate estimates of m in detail. Rather, we are concerned

[5] Although channel fading (due to multipath or shadowing effects) can be a significant source of errors for low E_b/N_o (i.e., energy per bit to noise spectral density ratio), multiple access interference (MAI) largely determines channel quality in non-orthogonally hopped FHMA systems.

[6] Of course, this assumes the transceivers are capable of supporting a sufficient range of code rates.

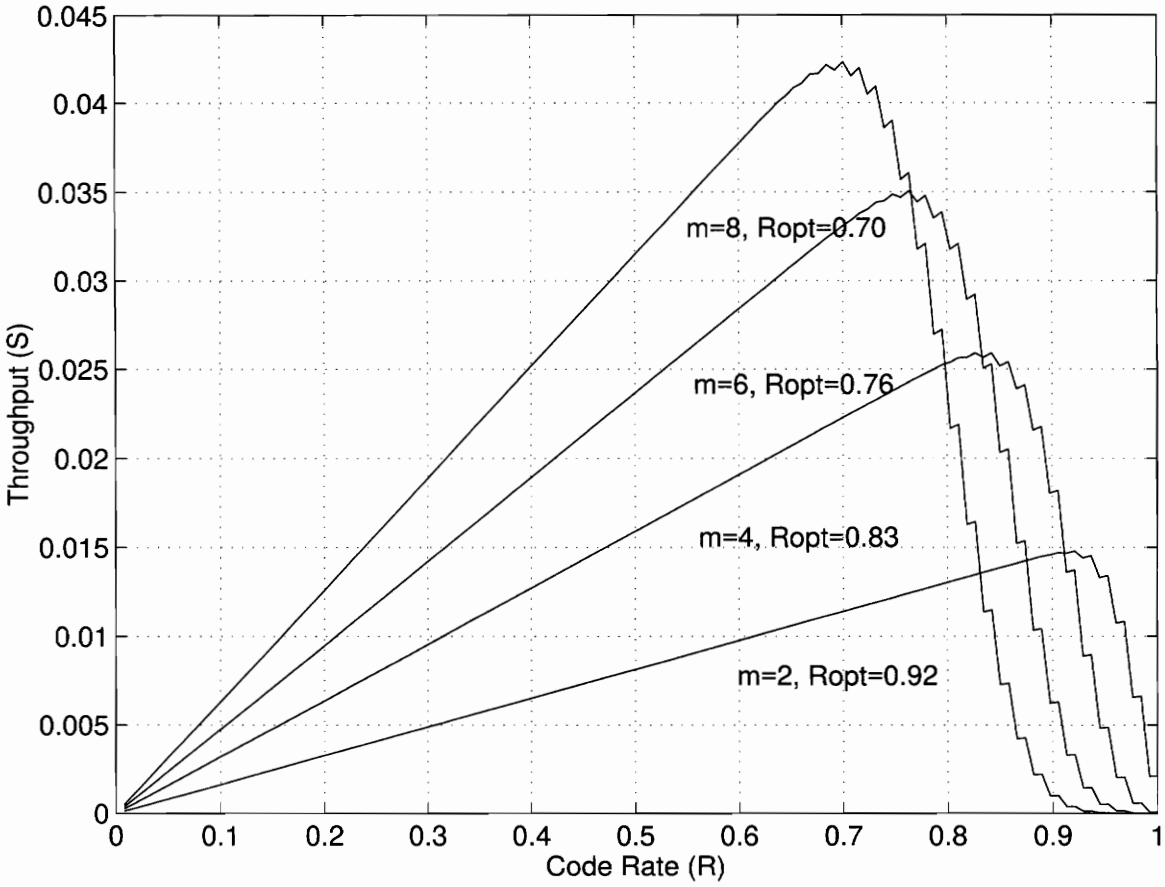

Figure 4.3: Throughput curves for m=2,4,6,& 8 users in an asynchronous hopped system showing that there is a unique optimal code rate for any particular system loading. (Results assume n=127 RS coding)

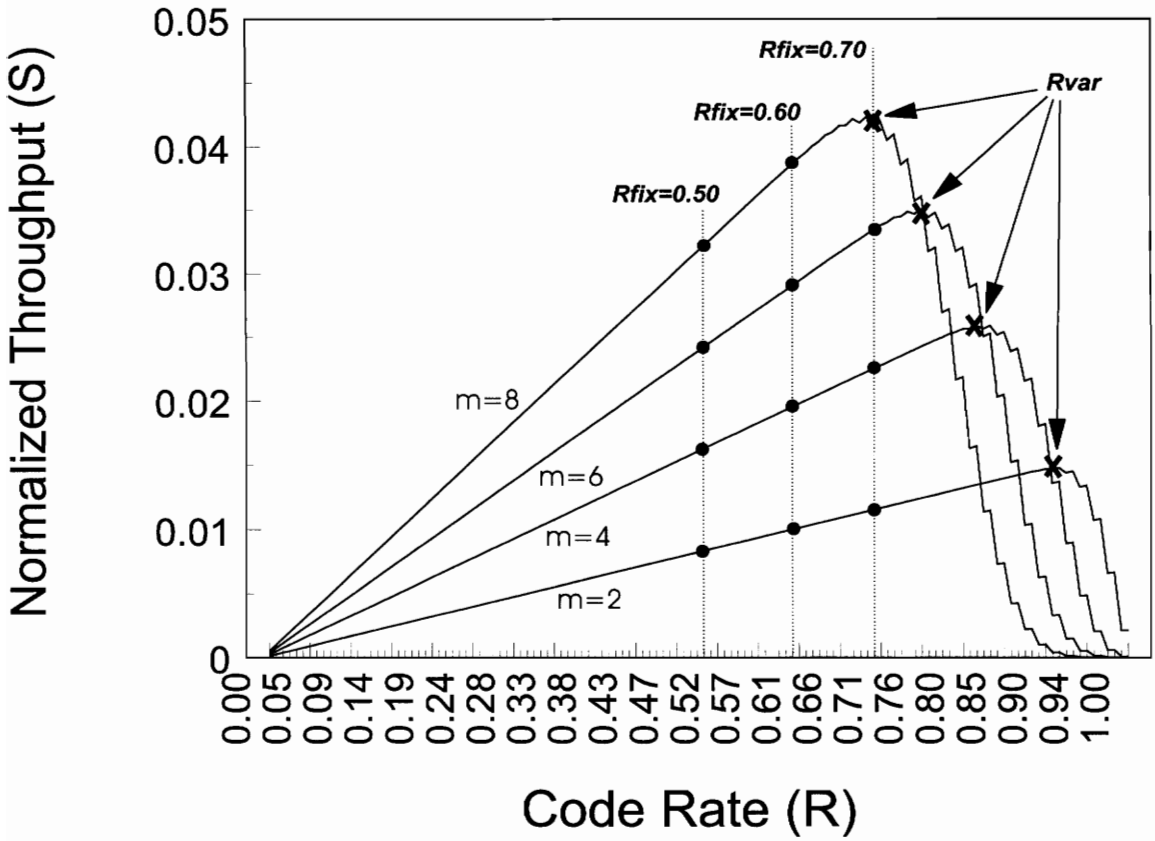

Figure 4.4: Comparing throughputs achievable with VRC as well as FRC in an Asynchronous No Side FHMA system with RS n=127 coding

Table 4.1: Comparison of FRC throughputs with optimal VRC throughput

# users	Peak S w/VRC	S w/R_{fix}=0.70 (% gain w/VRC)	S w/R_{fix}=0.60 (% gain w/VRC)	S w/R_{fix}=0.50 (% gain w/VRC)
m=2	.0148	0.0114 (+29.8%)	0.0098 (+51.0%)	0.0081 (+82.7%)
m=4	.0259	0.0222 (+16.7%)	0.0191 (+35.6%)	0.0159 (+62.9%)
m=6	.0350	0.0331 (+05.7%)	0.0284 (+23.2%)	0.0237 (+47.7%)
m=8	.0423	0.0423 (+ 0.0%)	0.0377 (+12.2%)	0.0315 (+34.3%)

with quantifying the potential throughput gains that VRC can offer to systems currently employing FRC techniques.

If a FRC scheme is to be used for the system configuration described in Figure 4.3 then the first step in the design would be to determine the maximum code rate (i.e., the weakest level of coding) that could be employed by the users in the system during worst case channel conditions. As an example, if it were known that there would never be more than m =8 active users in the system at any time, then the maximum code rate that would provide sufficient protection for up to 8 users in the system is R=0.70 (corresponding to the throughput peak of the m=8 curve in Figure 4.3). Therefore, a reasonable choice for a fixed code rate for the users in the system would be R=0.70 or less. Choice of R less than 0.70 would result in robustness to account for other channel effects (such as channel fading [7] or shadowing). Figure 4.4 shows a comparison of the peak throughputs achievable with VRC as well as with FRC schemes with code rates of R_{fix} =0.70, 0.60, & 0.50 for the loadings of m=2, 4, 6, &8 users. The peak throughputs achievable with VRC are indicated on each curve by "x"'s while black dots on the curves indicate the achievable throughputs with the three FRC schemes. Table 4.1 presents this same data in tabluar form where it is seen that VRC has the potential to provide significant gains when compared to FRC schemes.

The idea of Variable Rate Coding was first proposed by Wardhana and Woerner [16]. Their studies produced general conclusions that VRC could provide significant capacity

[7]We assume that the performance of FHMA systems employing non-orthogonal hopping is dominated by MAI rather than channel fading. This usually is not a reasonable assumption however, in other types of systems.

benefits to wireless FHMA systems. In this thesis, we undertake a more rigourous analysis of the idea of Variable Rate Coding and present throughput results for a variety of system conditions and configurations. We explore cases of synchronous and asynchronous hopping, availability/unavailability of collision information, and expected performance bounds of practical length RS block codes. We also present an analysis of the effects of channel fading on system throughput performance as well as an analysis of the required accuracy in estimates of m to achieve gains over practical FRC schemes.

Chapter 5

Analysis & Results

5.1 System Model and Performance Measures

The FHMA system under consideration is shown in Figure 5.1 and is composed of m independent transmitter-receiver pairs (or m users [1]) that communicate over a common channel. Each user in the system is given a specified pseudorandom code sequence which hops the user's carrier frequency among a set of q contiguous frequency slots. For all numerical examples in this thesis, we have assumed $q = 128$. The users in the system use M-ary Frequency Shift Keying (FSK) modulation. For simplicity we assume the FHMA system is a slow hopped system where exactly one symbol is transmitted during each hop interval. Both synchronous and asynchronous hopping are evaluated in this thesis.

The performance measure used in this thesis is average normalized system throughput. We define the system throughput with m simultaneously transmitting users $W(m) = m \cdot P_c(m)$ to be a measure of the total information flow in the system where $P_c(m)$ is the probability of receiving the correct code word given m transmitting users in the system. In order to form a basis to compare our FHMA system with other multiple-access systems we define normalized throughput given m users $S(m)$ to be the data throughput $W(m)$, normalized by the code rate R and number of frequency slots q, given by

$$S(m) = R \cdot W(m)/q = R \cdot m \cdot P_c(m)/q. \tag{5.1}$$

The number of users m is considered to be a random variable which is Poisson distributed

[1] In this thesis, the terms *user* and *transmitter-receiver pair* will be used interchangeably

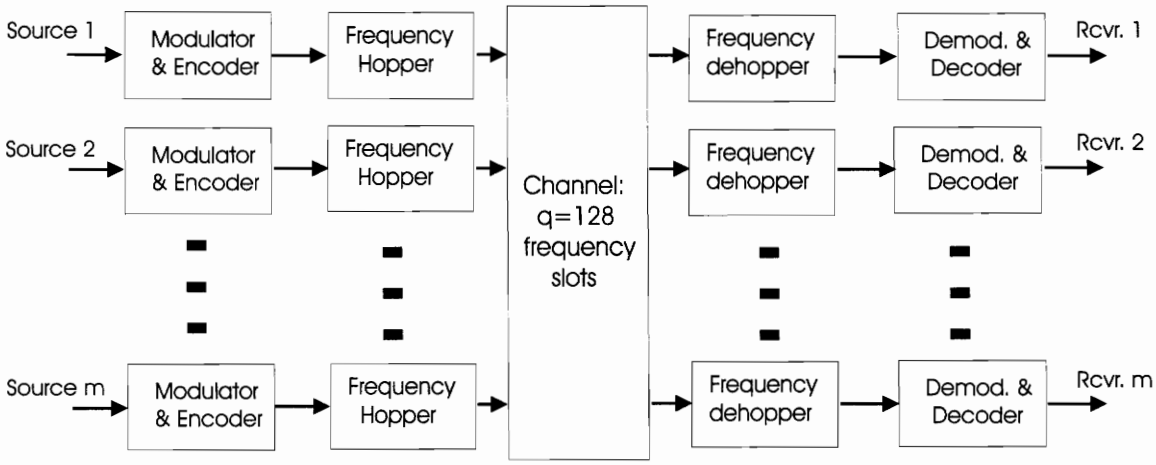

Figure 5.1: FHMA system with m transmitter/receiver pairs [4]

with an average value λ [2]. The expected normalized peak system throughput for a fixed code rate $R_{fix}(\lambda)$ is

$$S_{fix}(\lambda) = \sum_{m=0}^{\infty} p_M(m) \cdot S(m) \tag{5.2}$$

$$= \sum_{m=0}^{\infty} p_M(m) \cdot R_{fix}(\lambda) \cdot \frac{m \cdot P_c(m)}{q} \tag{5.3}$$

$$= \frac{R_{fix}(\lambda)}{q} \sum_{m=0}^{\infty} p_M(m) \cdot m \cdot P_c(m) \tag{5.4}$$

where $R_{fix}(\lambda)$ is the fixed code rate which maximizes system throughput when an average of λ users are present (i.e., the optimal fixed code rate for an average loading of λ users), and $p_M(m)$ is the Poisson distribution (or the probability of m users being present in the system at a given time),

$$p_M(m) = \frac{e^{-\lambda} \cdot \lambda^m}{m!}. \tag{5.5}$$

This throughput $S_{fix}(\lambda)$ will be compared to the throughput of a system with a variable code rate chosen to maximize throughput for each value of m. The expected normalized

[2] i.e. $\lambda = E[M]$ where M is a random variable representing the number of users in the system at a given time

system throughput is then

$$S_{var}(\lambda) = \frac{1}{q} \sum_{m} m \cdot p_M(m) \cdot R_{var}(m) \cdot P_c(m) \tag{5.6}$$

where $R_{var}(m)$ is the variable code rate which maximizes equation (1) for each individual m and S_{var} depends on λ since the user distribution $p_M(m)$ depends on λ.

5.2 Throughput Bounds of Variable Rate and Fixed Rate Coding Schemes when Coding at Capacity

This section derives throughput bounds for variable rate and fixed rate channel codes which achieve capacity. To attain these gains, channel capacity C is considered as opposed to a specific realizable code. It is assumed that for a given user population, the system will choose a code rate equal to C, thus always receiving the correct code word (i.e. $P_c(m) = 1$). To find the normalized throughput, we let $R = C$ and $P_c(m) = 1$ in equation (5.1). The capacity is dependent on the specific channel under consideration. Synchronous and asynchronous channels are examined.

This subsection presents the throughput bounds for a system using fixed rate coding as well as variable rate coding in a non-fading channel with and without the availability of side information. The latter part of this subsection then reexamines these throughput bounds for a Rayleigh fading channel where BFSK modulation is employed.

Perfect Side Information

Perfect side information (PS) is the case where the receiver always knows when a collision (i.e., hit) [14] has occured for each symbol. A collision or hit is the event when two or more users utilize the same frequency slot simultaneously resulting in a corrupted symbol. Perfect side information allows a receiver to label each hit symbol as an erasure [3]. We model this situation by a M-ary erasure channel, where M is the number of symbols used. For this channel the transmission probabilities are

$$P(y|x) = \begin{cases} 1 - p_{h,m} & y = x \\ p_{h,m} & y = erasure \\ 0 & else \end{cases} \tag{5.7}$$

[3]Labeling hit symbols as erasures may be pessimistic since it has been shown that under some circumstances automatically declaring an erasure is not optimal [26].

where y is the received symbol, x is the transmitted symbol, and $p_{h,m}$ is the probability of a hit given m users in the system. Additionally, it can be shown that

$$P(x|y) = \begin{cases} 1 & x = y \\ 1/M & y = erasure \\ 0 & else \end{cases} \tag{5.8}$$

assuming an equiprobable source symbol distribution.

The capacity of a channel is defined as the maximum mutual information transferred per use of the channel. It can be shown [27] that the channel capacity $C_{PS}(m)$ of an M-ary erasure channel with perfect side information and m users is

$$C_{PS}(m) = 1 - p_{h,m}. \tag{5.9}$$

Thus the normalized throughput for a given number of users is equal to,

$$S(m) = \frac{(1 - p_{h,m})m}{q} \tag{5.10}$$

where $p_{h,m}$ is dependent on the number of users in the system, m, and also whether synchronous or asynchronous hopping is employed. It has been shown in [28] that the probability of a hit in a synchronous system with m users is

$$p_{h,m} = 1 - \left(1 - \frac{1}{q}\right)^{m-1} \tag{5.11}$$

and the probability of a hit in an asynchronous system [4] with m users is approximated by

$$p_{h,m} \cong 1 - \left(1 - \frac{2}{q}\right)^{m-1}. \tag{5.12}$$

The expression for the optimal expected normalized throughput of a system that uses a fixed code rate is obtained by substituting (5.5) and $P_c(m) = 1$ into (5.4) resulting in

$$S_{fix}(\lambda) = R_{fix}(\lambda) \cdot \sum_{m=0}^{\lambda} \frac{e^{-\lambda} \cdot \lambda^m}{m!} \cdot \frac{m}{q}, \tag{5.13}$$

[4]The probability of a hit in an asynchronous system is greater than in a synchronous system because a given interferer may collide with the desired user during two hops instead of only one.

where $R_{fix}(\lambda)$ is the fixed code rate which results in optimum performance for an average loading of λ users in the system [15]. The summation extends to $m = \lambda$ since for any $m > \lambda$, $C_{PS}(m)$ would exceed the system's actual capacity. This set of values is compared to the optimal expected normalized throughput when a variable code rate is used based on a perfect estimate of the number of users in the system, m. This is given by substituting (5.5) and $P_c(m) = 1$ into (5.6) resulting in

$$S_{var}(\lambda) = \sum_{m=0}^{\infty} \frac{e^{-\lambda} \cdot \lambda^m}{m!} \cdot R_{var}(m) \cdot \frac{m}{q}, \tag{5.14}$$

where $R_{var}(m) = C_{PS}(m)$ is the code rate which optimizes throughput based on m users in the system.

The resulting optimal expected throughput of each channel is given in the upper two curves of Figure 5.2 for a synchronous system with perfect side information. The peak throughput for the synchronous system with perfect side information is 0.3025 at an average system loading of λ=118 users with optimized fixed rate coding (shown by the dotted curve) and 0.3679 [5] at an average system loading of λ=128 users with optimized variable rate coding (shown by the solid curve). Thus, optimized variable rate coding can provide 21.6% greater peak throughput over optimized fixed rate coding in a Synchronous, Perfect Side information system.

Throughput results for an asynchronous system with perfect side information system are given by substituting equation (5.12) in equation (5.9) and then combining this with equations (5.13) and (5.14) with $R_{var}(\lambda) = C_{PS}(\lambda)$ and $R_{fix}(\lambda)$ equal to the fixed code rate which optimizes throughput for an average loading of λ users in the system. Figure 5.2 shows that the peak normalized system throughput for the Asynchronous, Perfect Side information system is 0.1424 at an average loading of λ=58 users with optimized fixed rate coding and 0.1839 at an average loading of λ=64 users with optimized variable rate coding. Thus, optimized variable rate coding can provide 29.2% greater peak throughput over

[5] Note that in all cases the peak normalized system throughput will never exceed this limit of $e^{-1} = 0.3679$ as explained in [14]. This upper bound on normalized throughput for a FH/SS system will hold in all cases investigated in this thesis.

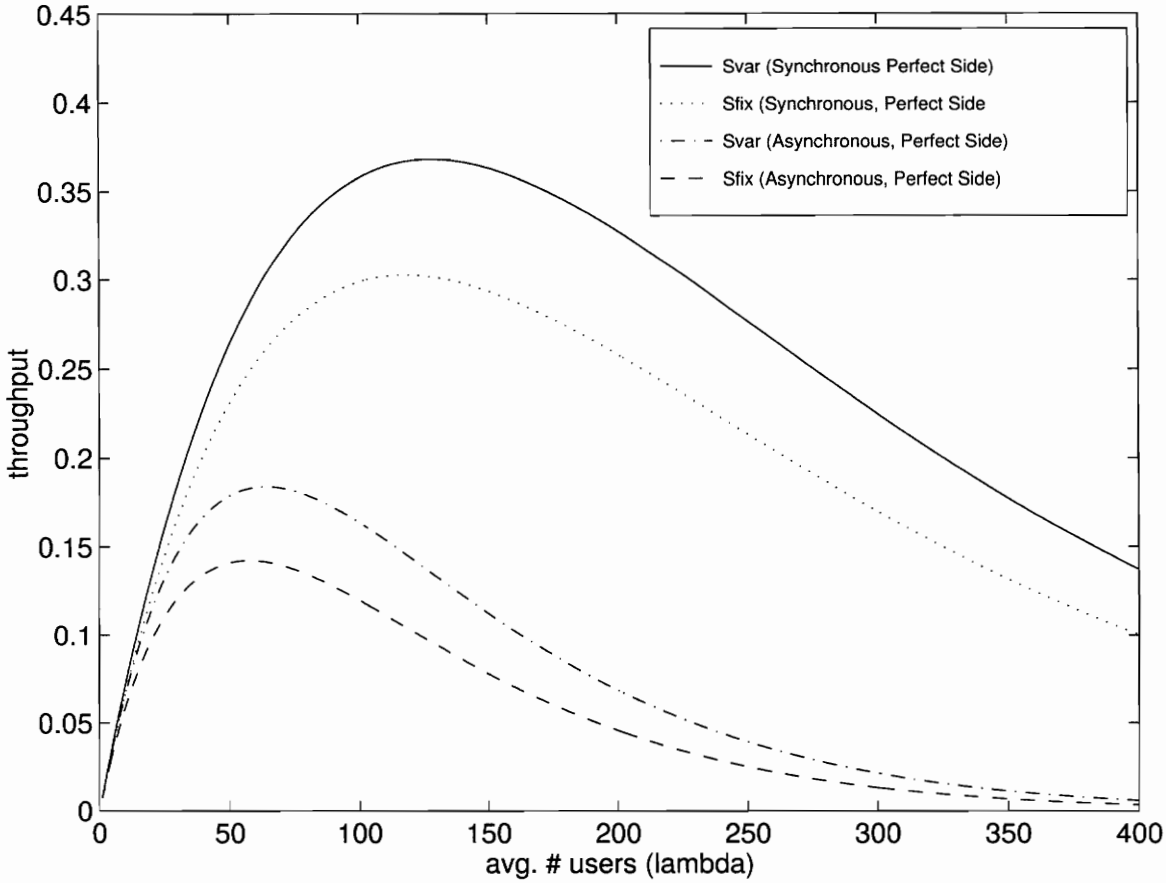

Figure 5.2: Throughput and potential gains when coding at capacity in a system with perfect side information (any M)

optimized fixed rate coding in an Asynchronous, Perfect Side information system (which is modestly higher than the percentage increase in throughput for the Synchronous, Perfect Side information system.

No side Information

The opposite extreme of the perfect side information case is the case where the receiver has no information about collisions. In this case, we consider a M-ary symmetric channel with transmission probabilities,

$$P(y|x) = \begin{cases} 1 - \left(\frac{M-1}{M}\right) \cdot p_{h,m} & x = y \\ \frac{p_{h,m}}{M} & \text{for the } M-1 \text{ cases where } x \neq y \end{cases} \tag{5.15}$$

with $P(x|y) = P(y|x)$ for an equiprobable source symbol alphabet. The channel capacity C_{NS} for the no side information case is given by

$$C_{NS} = 1 + \left(\frac{M-1}{M} \cdot p_{h,m} \cdot \log_M \left(\frac{p_{h,m}}{M}\right) + \left(1 - \frac{M-1}{M} \cdot p_{h,m}\right) \cdot \log_M \left(1 - \frac{M-1}{M} \cdot p_{h,m}\right)\right). \tag{5.16}$$

Again, $p_{h,m}$ is defined by (5.11) for synchronous systems or (5.12) for asynchronous systems.

The upper two curves of Figure 5.3 show that the peak throughput for the synchronous system with no side information is 0.1901 at an average loading of λ=82 users with optimized fixed rate coding or 0.2382 at an average loading of λ=89 users with optimized variable rate coding. Thus, optimized variable rate coding can provide 25% greater peak throughput over optimized fixed rate coding in a Synchronous, No Side information system. The bottom two curves in Figure 5.3 present the results for an asynchronous system with no side information where it is seen that the peak system throughput is 0.0890 at an average loading of λ=40 users for optimized fixed rate coding and 0.1193 at an average loading of λ=45 users for optimized variable rate coding. Thus, optimized variable rate coding provides 34.1% greater peak throughput than optimized fixed rate coding in an Asynchronous, No Side information system.

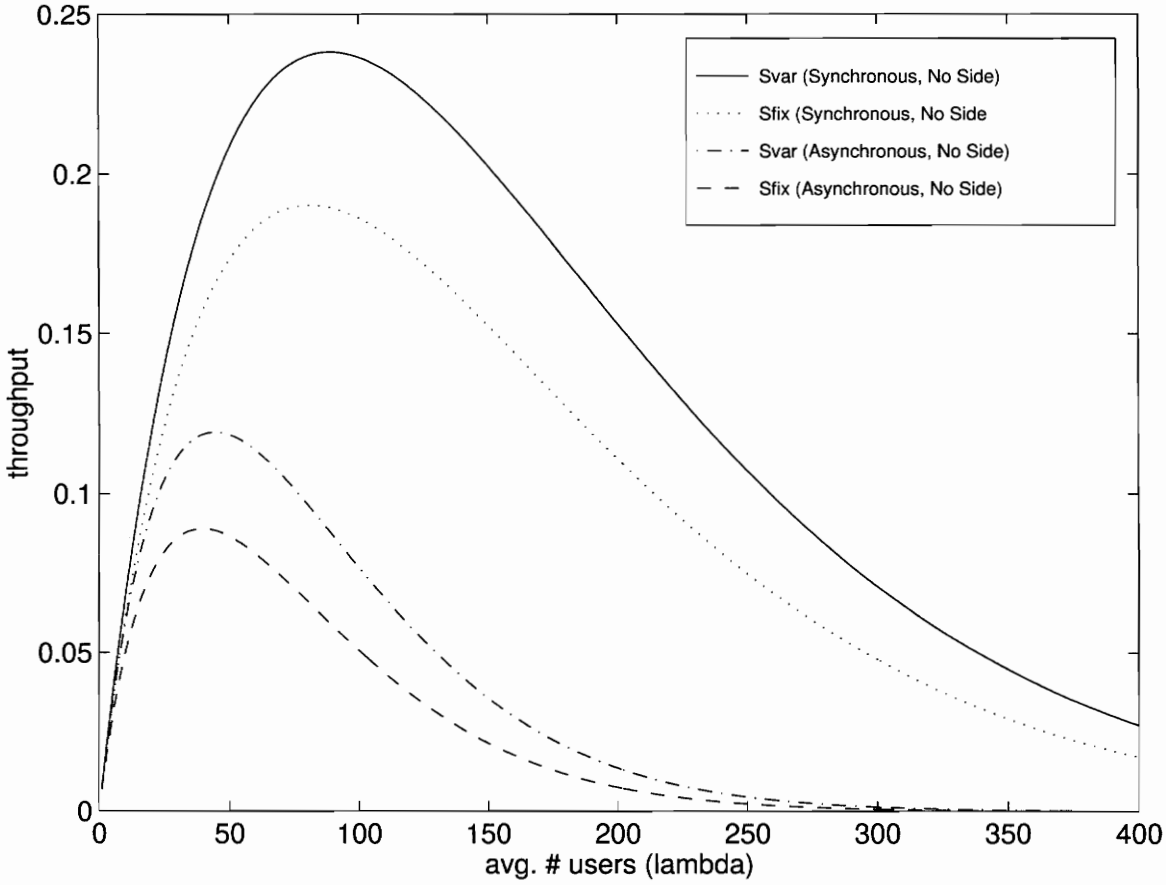

Figure 5.3: Throughput and potential gains when coding at capacity in a system with no side information (M=64)

Table 5.1: Throughput gains with variable rate coding when coding at capacity

System	M	Peak S w/variable R	Peak S w/fixed R	gain in S	% gain
Synch, PS	any M	0.3679 @ λ=128 users	0.3025 @ 118 users	+0.0653	+21.6 %
Synch, NS	64	0.2382 @ λ=89 users	0.1901 @ λ=82 users	+0.0481	+25.3 %
	128	0.2515 @ λ=93 users	0.2016 @ λ=85 users	+0.0499	+24.8 %
	256	0.2629 @ λ=97 users	0.2114 @ λ=89 users	+0.0515	+24.4 %
Asynch, PS	any M	0.1839 @ λ=64 users	0.1424 @ λ=58 users	+0.0416	+29.2 %
Asynch, NS	64	0.1193 @ λ=45 users	0.0890 @ λ=40 users	+0.0303	+34.1 %
	128	0.1260 @ λ=47 users	0.0945 @ λ=42 users	+0.0315	+33.3 %
	256	0.1316 @ λ=49 users	0.0991 @ λ=43 users	+0.0325	+32.8 %

In the four types of systems explored, the percentage gains are the greatest in the asynchronous system with no side information case because it is in this type of system that interference from other users is the most prominent and where coding is thus most helpful. Table 5.1 shows that percentage throughput gains when using variable rate coding at channel capacity remain relatively constant as M increases, although the absolute system throughput levels increase.

Optimized variable rate coding relies on perfect accuracy in the estimate of the number of users in the system, m, while fixed rate coding using a code rate $R_{fix}(\lambda)$ is optimized only when the average system loading is fixed at λ users. When considering the results presented for optimized fixed rate coding cases, it should be kept in mind that systems using a fixed rate code would rarely achieve their optimum throughput levels. This is because a code rate powerful enough to provide reasonable performance for the worst case loading of the system is usually chosen when fixed rate coding is employed rather than $R_{fix}(\lambda)$. Therefore although not shown in this thesis, it is intuitive that gains of a system using optimal variable rate coding versus a realistic (i.e., non-optimized) fixed rate coding scheme could be significantly higher than the gains represented by Table 5.1 for codes that achieve capacity.

Results for a Rayleigh Fading Channel

In mobile wireless channels, the assumption that multiple access interference dominates performance may no longer be valid since fading can be a significant source of symbol errors. Therefore, we extend the results of the previous two subsections and determine the performance of both optimal fixed rate and variable rate coding schemes in a Rayleigh fading channel.

In the presence of fading, our definition of Perfect Side information is expanded to include knowledge of faded symbols [20] as well as hit symbols. A *faded symbol* is a symbol that cannot be reliably decoded because of severe channel attenuation.

Our expanded definition of Perfect Side information allows a receiver to label faded symbols as erasures as well as hit symbols. Thus our M-ary channel transmission probabilities described in equations (5.7) and (5.15) are modified to

$$P(y|x) = \begin{cases} 1 - p_{se} & y = x \\ p_{se} & y = \text{erasure} \\ 0 & \text{else} \end{cases} \tag{5.17}$$

for a Perfect Side information system or

$$P(y|x) = \begin{cases} 1 - \left(\frac{M-1}{M}\right) \cdot p_{se} & x = y \\ \frac{p_{se}}{M} & \text{for the } M-1 \text{ cases where } x \neq y \end{cases} \tag{5.18}$$

for a No Side information system where p_{se} is the probability of a symbol error defined as

$$p_{se} = p_{se,f} + (1 - p_{se,f}) \cdot p_{h,m} \tag{5.19}$$

where $p_{se,f}$ is the probability of a symbol error due to the fading process independent of multiple access interference.

The capacity of the channel is redefined as

$$C'_{PS}(m) = 1 - p_{se}. \tag{5.20}$$

for a Perfect Side information system and

$$C'_{NS} = 1 + \left(\frac{M-1}{M} \cdot p_{se} \cdot \log_M \left(\frac{p_{se}}{M}\right) + \left(1 - \frac{M-1}{M} \cdot p_{se}\right) \cdot \log_M \left(1 - \frac{M-1}{M} \cdot p_{se}\right)\right). \tag{5.21}$$

for a No Side information system.

Expressions for the expected normalized throughput in a Rayleigh fading channel can be obtained by substituting new expressions for $R_{fix}(\lambda)$ and $R_{var}(m)$ into equations (5.13) and (5.14). In the Rayleigh fading case, $R_{fix}(\lambda)$ is redefined to be the fixed code rate which results in optimum performance for an average loading of λ users in the system and a given p_{se} and $R_{var}(m)$ is redefined to be equal to C'_{PS} for Perfect Side information systems or C'_{NS} for No Side information systems.

To generate performance results, we assume Binary FSK (BFSK) modulation as well as sufficient code symbol interleaving to allow burst errors to be dispersed into more random patterns. It is shown in [18] that

$$p_{se,f} = \frac{1}{2 + \frac{E_b}{N_o}} \tag{5.22}$$

for BFSK in a frequency-nonselective Rayleigh fading channel with a noncoherent demodulator.

Figure 5.4 shows the peak performance of Perfect Side and No Side information systems using codes that achieve capacity in a Rayleigh flat fading channel relative to the non-fading channel for a range of E_b/N_o from 1 to 30 dB. The Figure indicates that the peak throughput levels of synchronous and asynchronous hopped systems degrade identically in the fading channel (compared to their relative performance in the non-fading channel). Thus there is a single curve in the Figure describing performance of the Synchronous Perfect Side and Asynchronous Perfect Side information systems as well as a single curve describing the performance of the Synchronous No Side and Asynchronous No Side information systems in the fading channel. From the two curves in the Figure, it is seen that the degradation of peak throughput in No Side information systems is more serious than in Perfect Side information systems. Figure 5.4 shows that for an E_b/N_o of 30 dB, the peak system throughput is

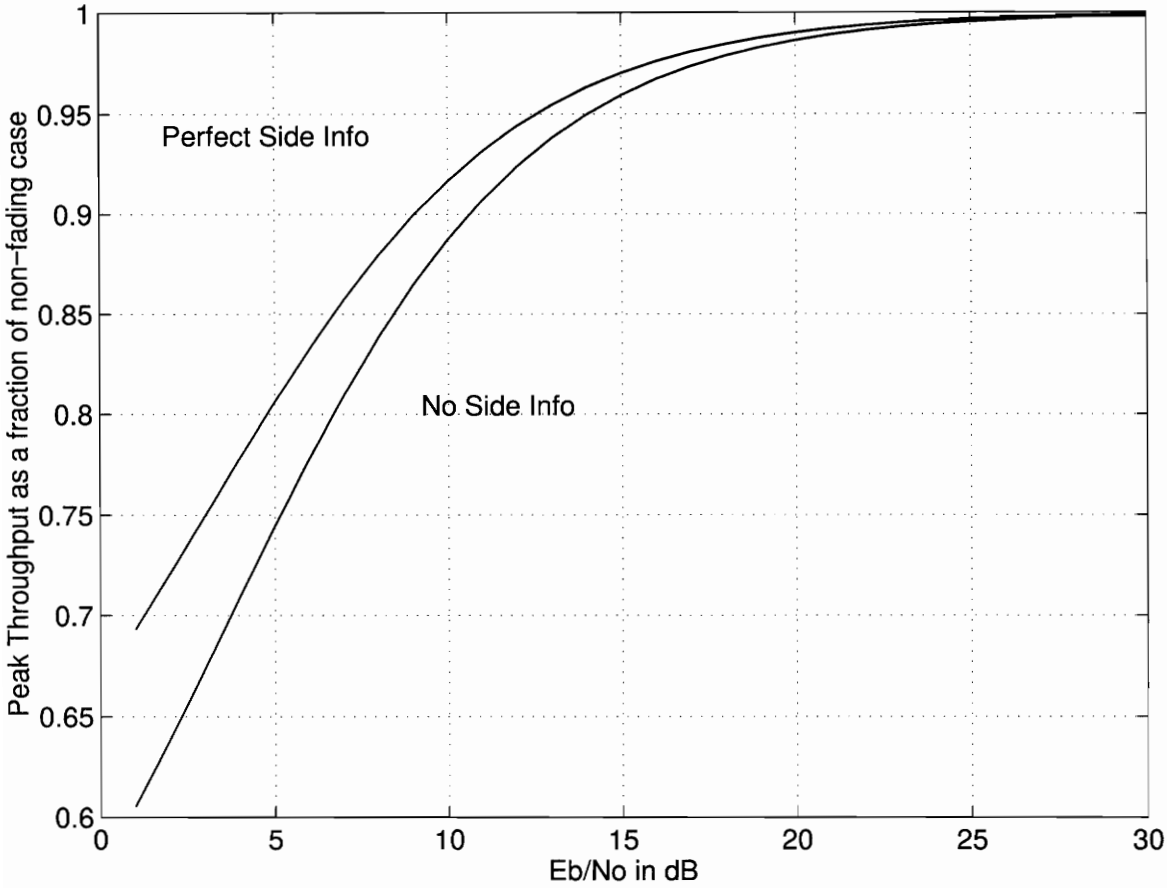

Figure 5.4: Peak throughput vs. E_b/N_o in a Rayleigh fading channel when using codes that achieve capacity in systems with and without side information

nearly identical to the non-fading cases in all four system configurations (ie., synchronous and asynchronous systems with or without side information). Another conclusion which can be drawn from the Figure is that multiple access interference no longer dominates system performance apart from channel fading for E_b/N_o below about 15 dB.

5.3 Throughput Bounds of Variable Rate and Fixed Rate Reed-Solomon Coding Schemes

Up until this point, we have considered perfect codes. This section investigates the throughput bounds of a system employing variable rate and fixed rate Reed-Solomon (RS) coding with practical block lengths of n=63, n=127, and n=255. RS codes are a special class of nonbinary BCH codes which achieve the largest possible minimum distance d_{min} of any linear code with the same encoder input and output lengths. An (n, k) RS code has a block length of n symbols. A number k of these symbols are information symbols and the remaining $n - k$ symbols are parity check digits. For an RS code, d_{min} can be specified as

$$d_{min} = n - k + 1. \tag{5.23}$$

RS codes can correct up to $d = n - k$ erasures or $t = \lfloor (n-k)/2 \rfloor$ errors where $\lfloor \cdot \rfloor$ is the greatest integer operator. Therefore, RS codes (regardless of code block length n) can correct approximately twice as many erasures as errors.

This subsection presents the throughput bounds for a system using fixed rate RS coding as well as variable rate RS coding in a non-fading channel with and without the availability of side information. The latter part of this subsection then reexamines these throughput bounds for the case of a Rayleigh fading channel where BFSK modulation is used.

Perfect Side Information

For the case of a non-fading channel, multiple access interference determines system performance. Perfect side information in such a channel means that the receiver has access to collision information thus allowing it to utilize the erasure correction capability of the code. In this case the probability of correct code word reception is

$$P_c(m) = \sum_{j=0}^{n-k} \binom{n}{j} p_{h,m}(m)^j \cdot (1 - p_{h,m}(m))^{n-j}, \tag{5.24}$$

where the probability of a hit $p_{h,m}$ is specified as (5.11) for synchronous systems and (5.12) for asynchronous systems. If we substitute equation (5.24) into equation (5.1) and subsequently take the expected value over the distribution $p_M(m)$ we can obtain the expression for the expected normalized system throughput $S(\lambda)$ for an arbitrary code rate R

$$S(\lambda) = \sum_{m=0}^{\infty} p_M(m) \frac{R \cdot m}{q} \sum_{j=0}^{n-k} \begin{pmatrix} n \\ j \end{pmatrix} p_{h,m}(m)^j \cdot (1 - p_{h,m}(m))^{n-j}. \tag{5.25}$$

From this equation, we define the expected normalized throughput for a system using an optimized variable code rate as

$$S_{var}(\lambda) = \sum_{m=0}^{\infty} p_M(m) \frac{R_{var}(m) \cdot m}{q} \sum_{j=0}^{n-k} \begin{pmatrix} n \\ j \end{pmatrix} p_{h,m}(m)^j \cdot (1 - p_{h,m}(m))^{n-j} \tag{5.26}$$

where again $R_{var}(m)$ is chosen to maximize (1) for any value of users in the system m and S_{var} depends on λ since $p_M(m)$ depends on λ. For a system using an optimized fixed code rate, the expected normalized throughput is

$$S_{fix}(\lambda) = R_{fix}(\lambda) \sum_{m=0}^{\infty} p_M(m) \frac{m}{q} \sum_{j=0}^{n-k} \begin{pmatrix} n \\ j \end{pmatrix} p_{h,m}(m)^j \cdot (1 - p_{h,m}(m))^{n-j} \tag{5.27}$$

where $R_{fix}(\lambda)$ is chosen to optimize throughput for an average of λ users.

The upper two curves in Figure 5.5 show that a sychronous system with perfect side information using RS coding with code length n=255 can achieve a peak normalized system throughput of 0.2865 at an average system loading of λ=113 users using optimized fixed rate coding or 0.3072 at an average loading of λ=114 users with optimized variable rate coding. Thus optimized variable rate coding provides 7.2% greater peak throughput than optimized fixed rate coding in a Synchronous, Perfect Side information system with n=255 RS coding. The bottom two curves in Figure 5.5 show that an asynchronous system with perfect side information using RS coding with n=255 can achieve a peak normalized system throughput of 0.1366 at an average system loading of λ=56 users using optimized fixed rate coding or 0.1537 at an average loading of λ=57 users using optimized variable rate coding.

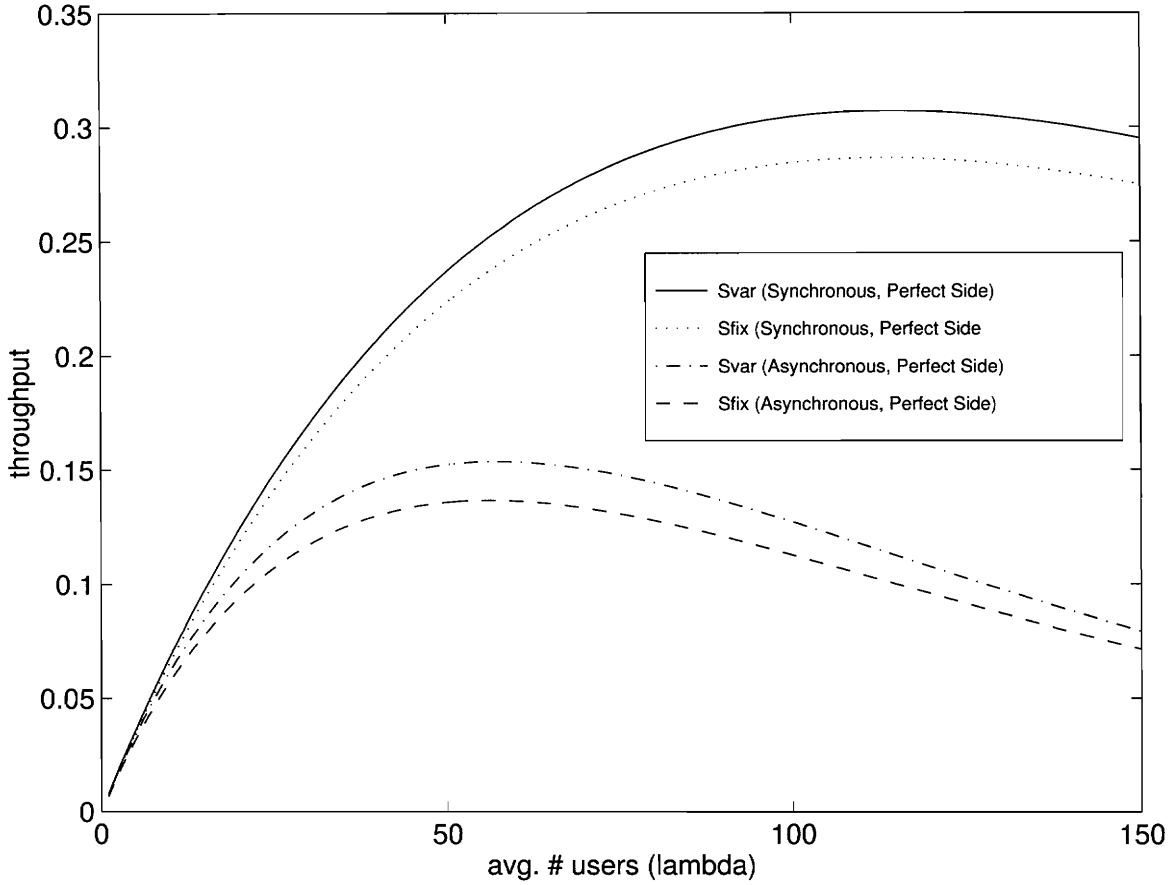

Figure 5.5: Throughput gains in synchronous and asynchronous systems with perfect side information and RS code length n=255

This amounts to a 12.5% greater peak throughput when comparing optimized variable rate coding to optimized fixed rate coding in an Asynchronous, Perfect Side information system with n=255 RS coding.

Results for systems using RS code lengths of n=63 and n=127 are presented in Table 5.2. The curves for these cases are very similar to the n=255 case. From the tabulated results it is seen that the gains due to variable rate coding increase as the code length, n, increases. In fact, the peak throughput gains achieved by optimized variable rate coding over optimized fixed rate coding approximately doubles as the code length is increased from n=63 to n=255. [14] and [15] suggest that as the RS code length is increased to infinity

Table 5.2: Throughput Gains when Comparing Optimized VRC to Optimized FRC using Reed Solomon coding with code lengths n=63,127, and 255.

System	n	Peak S with optimized VRC	Peak S with optimized FRC	gain in S gain in S	% gain % gain
Synch, PS	63	0.2774 @ λ=108 users	0.2646 @ λ=108 users	+0.0090	+3.4 %
	127	0.2912 @ λ=111 users	0.2769 @ λ=111 users	+0.0143	+5.2 %
	255	0.3072 @ λ=114 users	0.2865 @ λ=113 users	+0.0207	+7.2 %
Synch, NS	63	0.1002 @ λ=34 users	0.0951 @ λ=34 users	+0.0051	+5.4 %
	127	0.1070 @ λ=34 users	0.0985 @ λ=34 users	+0.0084	+8.6 %
	255	0.1139 @ λ=35 users	0.1015 @ λ=34 users	+0.0124	+12.2 %
Asynch, PS	63	0.1369 @ λ=54 users	0.1286 @ λ=53 users	+0.0083	+6.5 %
	127	0.1457 @ λ=56 users	0.1333 @ λ=57 users	+0.0124	+9.3 %
	255	0.1537 @ λ=57 users	0.1366 @ λ=56 users	+0.0170	+12.5 %
Asynch, NS	63	0.0504 @ λ=17 users	0.0458 @ λ=17 users	+0.0045	+9.9 %
	127	0.0537 @ λ=17 users	0.0467 @ λ=16 users	+0.0070	+15.0 %
	255	0.0571 @ λ=18 users	0.0475 @ λ=17 users	+0.0096	+20.1 %

the results for the RS cases will approach the bounds given in Section 2.

No Side Information

For the case of no side information, we must rely on the error correcting capability of the RS code rather than its erasure correction capability. Since the code can correct only half as many errors as erasures, the probability of receiving the correct code word and the expected normalized throughput for variable and fixed rate coding are found by changing the upper bound on the summations for j in equations (5.24), (5.26), and (5.27) from $n-k$ to $\lfloor \frac{n-k}{2} \rfloor$.

The results for a synchronous system with no side information with RS code length n=255 are presented in the upper two curves of Figure 5.6. The peak normalized system throughput is 0.1015 at an average system loading of λ=34 users for optimized fixed rate coding or 0.1139 at an average loading of λ=35 users for optimized variable rate coding. Thus, variable rate coding provides 12.2% greater peak throughput over optimized fixed

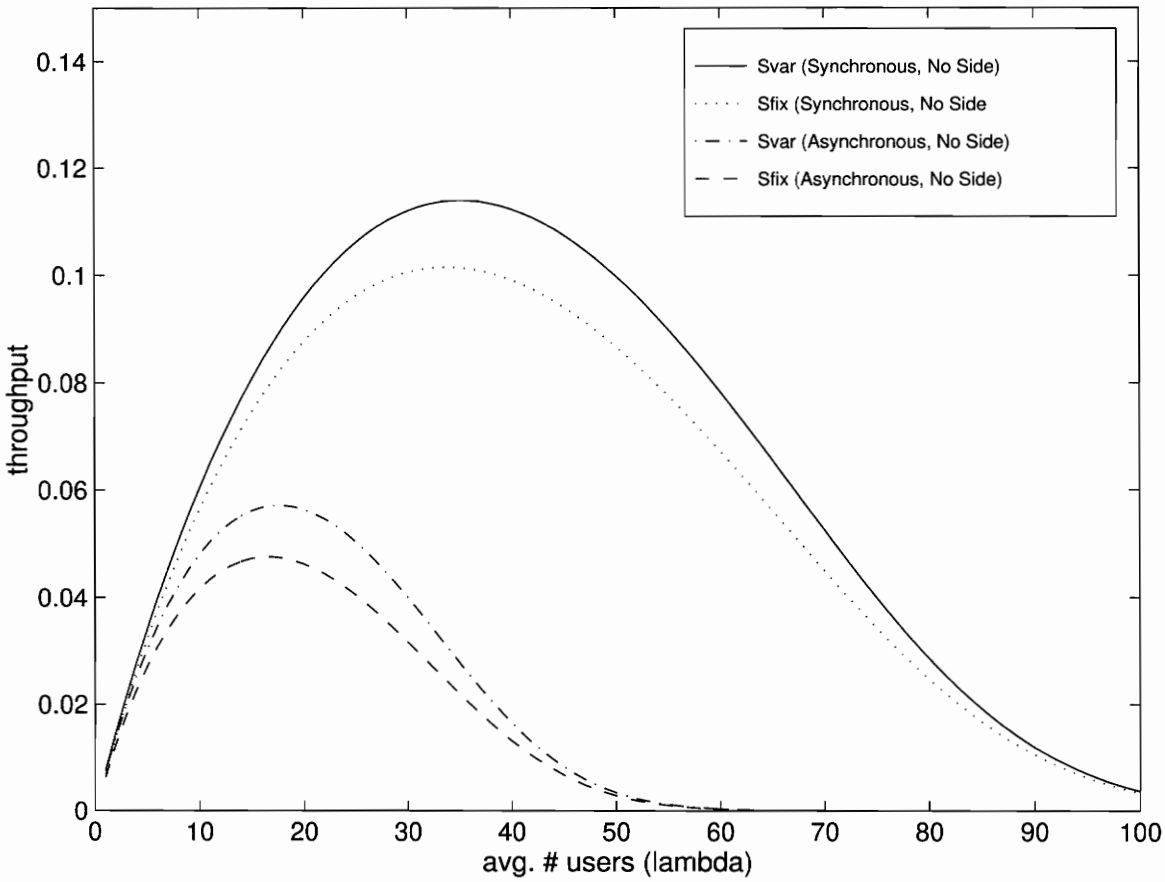

Figure 5.6: Throughput gains in synchronous and asynchronous systems with no side information and RS code length n=255

rate coding for the Synchronous, No Side information system. The bottom two curves of Figure 5.6 show that the gains due to variable rate coding in an asynchronous system with no side information are even greater. The peak normalized system throughput in this system is 0.0475 at an average of λ=17 users for optimized fixed rate coding and 0.0571 at an average of λ=18 users for optimized variable rate coding which calculates to 20.1% greater peak throughput when comparing the optimized variable rate coding case to the optimized fixed rate coding case.

Results for no side information systems using RS codes of lengths n=63 and n=127 are tabulated in Table 5.2 along with the results for the perfect side information systems. As

was observed in the perfect side information cases, the throughput gains due to variable rate coding increase with the code length n and are approximately doubled as the code length is increased from n=63 to n=255.

The Effect of Rayleigh Fading on Variable Rate and Fixed Rate RS Coding Throughput Bounds

Subsections 4.1 and 4.2 presented the throughput bounds for the four system types in a non-fading channel. In this subsection we reexamine the throughput bounds for fixed rate and variable rate n=127 Reed-Solomon coding schemes for all four system types (i.e, synchronous & asynchronous hopped systems with and without side information) in a Rayleigh flat fading channel. As was the case in subsection 3.3, our definition of Perfect Side information includes the knowledge of faded symbols as well as hit symbols. The M-ary channel transmission probabilities remain as given by equation (5.17) for Perfect Side information systems and equation (5.18) for No Side information systems. The probability of a symbol error is given by (5.19) and is equal to

$$p_{se} = \frac{1}{2+\frac{E_b}{N_o}} + \left(1 - \frac{1}{2+\frac{E_b}{N_o}}\right) \cdot p_{h,m} \tag{5.28}$$

for BFSK modulation in a frequency-nonselective Rayleigh fading channel with a noncoherent demodulator where $p_{h,m}$ is given by (5.11) for synchronous systems and (5.12) for asynchronous systems.

The probability of receiving a correct code word then becomes

$$P_c(m) = \sum_{j=0}^{n-k} \binom{n}{j} p_{se}(m)^j \cdot (1 - p_{se}(m))^{n-j}, \tag{5.29}$$

for a perfect side information system. Substituting equation (5.29) into equation (5.1) gives us the expressions for the expected normalized system throughput $S(\lambda)$ which can then be expressed as

$$S_{var}(\lambda) = \sum_{m=0}^{\infty} p_M(m) \frac{R_{var}(m) \cdot m}{q} \sum_{j=0}^{n-k} \binom{n}{j} p_{h,m}(m)^j \cdot (1 - p_{h,m}(m))^{n-j} \tag{5.30}$$

for a perfect side information system employing variable rate coding and

$$S_{fix}(\lambda) = R_{fix}(\lambda) \sum_{m=0}^{\infty} p_M(m) \frac{m}{q} \sum_{j=0}^{n-k} \begin{pmatrix} n \\ j \end{pmatrix} p_{h,m}(m)^j \cdot (1 - p_{h,m}(m))^{n-j} \tag{5.31}$$

for a perfect side information system employing fixed rate coding. The expressions for the no side information case are identical to (5.29), (5.30) and (5.31) except that the upper limit for the summations for j changes from $n-k$ to $\lfloor \frac{n-k}{2} \rfloor$.

Figure 5.8 shows the performance bounds for Perfect Side and No Side information systems using perfectly interleaved (i.e., no bursts of symbol errors) n=127 RS codes in a Rayleigh fading channel relative to the non-fading channel results obtained in the previous two subsections. The throughput bounds for synchronous and asynchronous hopped systems degrade identically (relative to their respective non-fading bounds) in both the Perfect Side and No Side information cases. As was observed in the case with perfect codes, performance in the fading channel is nearly identical to the non-fading channel for high signal to noise ratios (i.e, an E_b/N_o of 30 dB or higher in these cases). The dashed curves represent the performance of the optimized variable rate coding schemes as compared to the performance of the schemes in the non-fading analysis. It is interesting to note that for n=127 RS codes, the optimized variable rate scheme degrades slightly more than the optimized fixed rate scheme for equivalent E_b/N_o. The relative percentage gains of optimzed VRC schemes over optimized FRC schemes in a Rayleigh fading channel with BFSK modulation are shown in Figure 5.7 where it is seen that the percentage gains begin to decline somewhat for E_b/N_o below 15 dB.

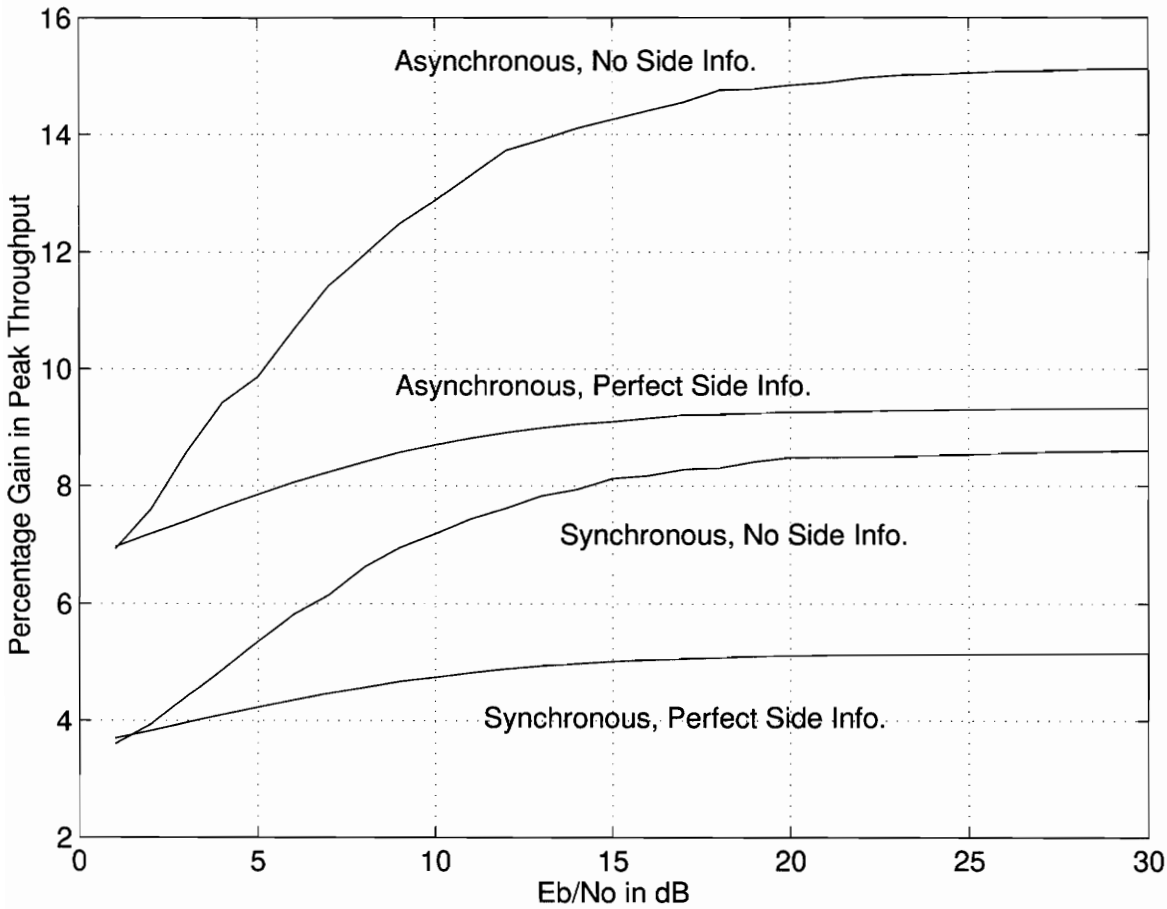

Figure 5.7: Percentage Throughput Gains of Optimized Variable Rate RS Coding when compared to Optimized Fixed Rate RS Coding (n=127) in a Rayleigh Fading channel.

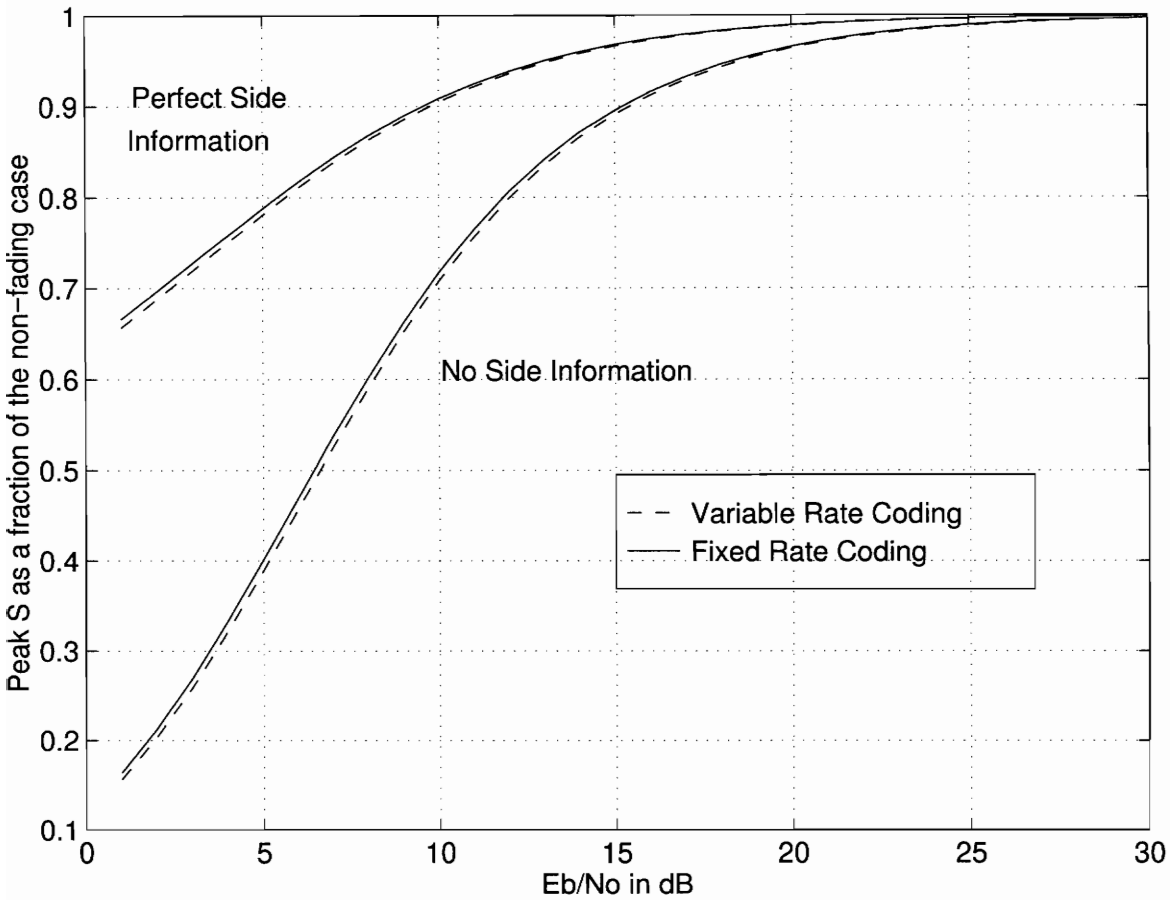

Figure 5.8: Peak Throughput vs. E_b/N_o in a Rayleigh fading channel for an n=127 RS code in systems with and without side information

5.4 Effect of Imperfect System Loading Estimates

The results of the previous sections provided bounds on the obtainable throughputs for fixed rate coding (FRC) and variable rate coding (VRC) schemes assuming a known fixed user population mean in the FRC cases (for which the optimal fixed code rate was chosen) and perfect estimates of m in the VRC cases. These assumptions were necessary to evaluate the bounds for throughput performance of the various systems but are not realistic in practical systems. In particular, the user population mean would not be constant in a wireless network but rather would change (e.g., between peak hours and non-peak hours) thus making it impossible to use a fixed code rate which could optimize throughput at all times in the FRC cases. Also, it is highly unlikely that perfect estimates of m will be avilable in a decentralized system thus invalidating the assumption made in calculating the bounds for the VRC cases. This section addresses the degradation in system throughput when these assumptions are removed. In particular we examine the throughput performance of an n=127 RS FRC scheme when the user population is 0% to 30% less than the design target mean (i.e., the average loading λ_{des} for which the fixed code rate $R_{fix}(\lambda_{des})$ maximizes throughput). Additionally, the effect of population estimation error on an n=127 RS VRC scheme is also investigated.

A system using FRC is normally designed to employ a code rate low enough (i.e., powerful enough) to provide sufficient error correction capability for the worst case channel conditions [6]. For example, if a certain system normally experiences mean loadings of λ=8 users in the morning hours, λ=10 users in the afternoon hours and λ=7 users in the evening hours, then the tranmitters should be configured to use a fixed code rate no higher than $R_{fix}(\lambda_{des} = 10)$ (i.e., the code rate which provides sufficient error correction for any λ up to 10 users but provides optimal throughput only for an average loading of λ=10 users [7]).

[6] Neglecting to design an FRC scheme for the worst case channel conditions runs the risk of severely degraded performance during periods when the channel produces enough errors to exceed the error correction capabilities of the code.

[7] Choosing a λ_{des} less than 10 (or equivalently, choosing a code rate greater than $R_{fix}(\lambda_{des} = 10)$) would not provide suffiecent error correction during periods when $\lambda > \lambda_{des}$.

In this case, optimal throughput would occur during the afternoon hours while non-optimal performance would occur during the other periods of the day. A more robust system design would be to choose $\lambda_{des} > 10$ users to allow a margin for unusually heavy loading or other sources of symbol errors (in cases where multiple access interference does not dominate performance). The choice of a λ_{des} which provides sufficient coding gain for the worst case channel conditions leads to non-optimized throughput for the FRC system during any periods that the user population mean is less than λ_{des}. The horizontal lines in Figure 5.9 show the peak throughput performance of an n=127 RS FRC scheme in an Asynchronous, Perfect Side information system when the user population mean is between 70% and 100% of the λ_{des}. The Figure shows that throughput decreases from a peak of 0.1333 in the case where $\lambda = \lambda_{des}$ (i.e., equivalent to the optimal FRC case) to 0.1289, 0.1178, and 0.1033 in the cases where λ is 90%, 80%, and 70% of the λ_{des} respectively. Thus when compared to the optimal VRC throughput of 0.1457 found in the earlier section, the potential gain in throughput with VRC can be as high as 13.0%, 23.7%, or 41.0% when λ is 90%, 80%, and 70% of the λ_{des} respectively. From these results it is obvious that n=127 RS VRC can provide much higher relative gains when compared to realistic (i.e., non-optimized) FRC schemes rather than the 9.3% gain suggested by our earlier comparison against optimal FRC.

The curve in Figure 5.9 illustrates the degradation of throughput for the n=127 RS VRC scheme when the estimates of m[8] are imperfect. From the curve it is seen that throughput degrades much more gracefully for estimates of m which are higher than the actual m rather than for estimates which are lower than the actual m. This is due to the

[8]It is possible that the receivers could obtain these estimates of m by monitoring the activity levels in a fixed number of frequency slots and relating the measured activity to m or alternatively by using a blind estimation algorithm where upon commencement of communication, the transmitter incrementally increases the transmission code rate from some nominal rate until the receiver measures that increasing throughput no longer occurs. From this information, it is possible to identify approximately where the throughput peak (and thus the optimal code rate $R_{var}(m)$) occurs. However, it is not our intention to analyze in detail the issue of obtaining accurate estimates of m in this thesis. Our main intention is to explore the performance benefits of variable rate coding assuming some method could be devised to provide reasonably accurate estimates of m.

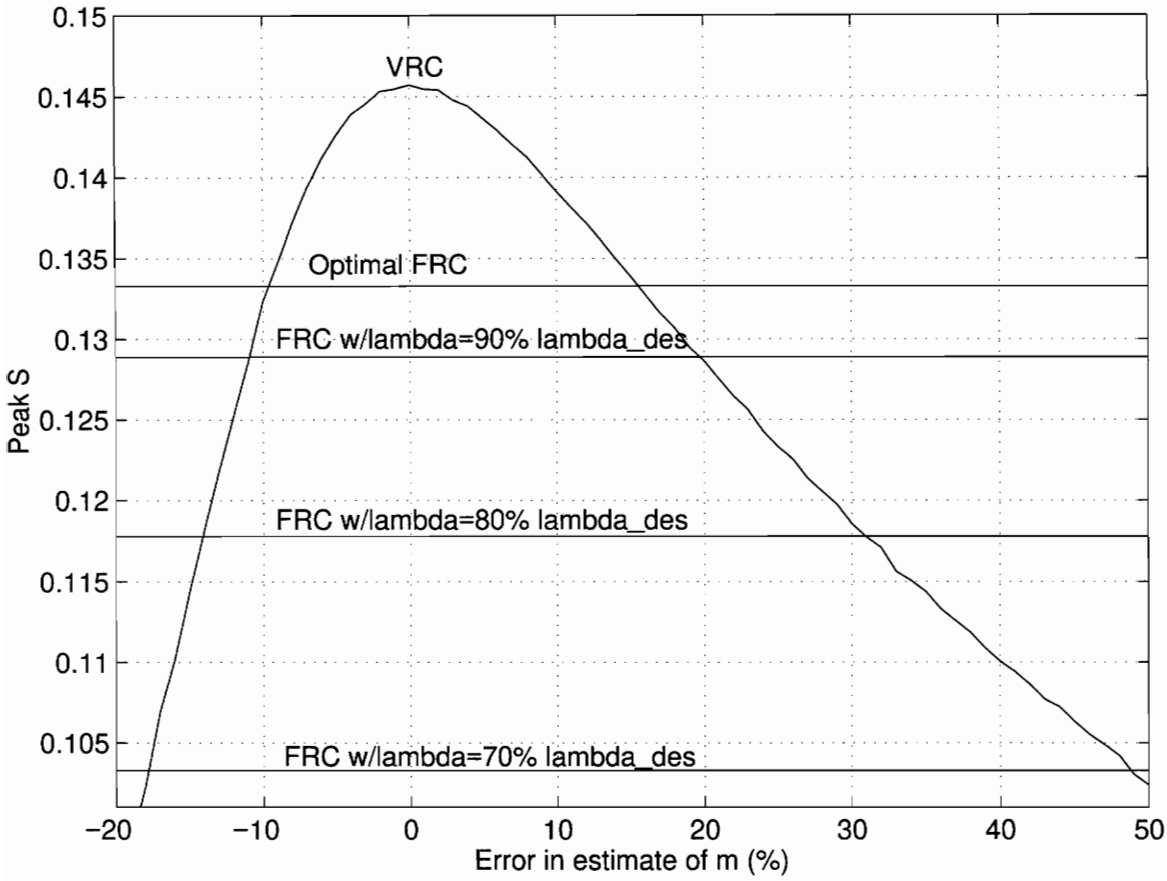

Figure 5.9: Peak Throughput in an Asynchronous, PS system using Variable Rate RS Coding (n=127)with Estimate Errors in m

fact that underestimating m would lead the m transmitter/receiver pairs in the system to use a weaker (i.e., higher) code rate than is necessary to overcome the level of interference produced by the m users in the system[9]. For example, a -15% error in the estimate of m results in a throughput loss of about -0.028 (when compared to the optimal VRC throughput of 0.1457) whereas a +15% error in the estimate of m resulrts in a less severe throughput loss of about -0.012. The intercepts of the VRC throughput curve with the horizontal lines illustrate the minimum required accuracies in the estimates of m for a VRC scheme to provide superior performance to an FRC scheme. For example, Figure 5.9 shows that if the estimates of m are within an accuracy of -17.8% to +48.8% then the n=127 RS VRC scheme will provide superior performance to a n=127 RS FRC scheme if $\lambda \leq 0.7 \cdot \lambda_{des}$. Alternatively, if the estimates of m are within an accuracy of -9.6% to +15.5% then the n=127 RS VRC scheme will always outperform the n=127 RS FRC scheme.

The results for the Asynchronous No Side, Synchronous Perfect Side, and Synchronous No Side information systems are summarized in Table 5.3. It is notable that in all four systems considered, the throughput benefits of using VRC can be on the order of 25% to 40% or more if comparison is made to non-optimal FRC schemes.

[9]The performance of a coded system degrades rapidly when the error correcting capability of the code is exceeded.

Table 5.3: Throughput Gains with VRC Compared to Non-Optimal FRC (and Required Accuracy in Estimates of m) using n=127 RS codes

System	FRC with code rate $R_{fix}(\lambda)$ code rate $R_{fix}(\lambda)$	Required accuracy in estimates of m to achieve gain over FRC	Potential Gains with VRC
Synch, PS	$\lambda = \lambda_{des}$	-7.5% & +10.8%	up to +5.2%
	$\lambda = 90\%\lambda_{des}$	-9.6% & +15.5%	up to +9.0%
	$\lambda = 80\%\lambda_{des}$	-13.4% & +27.7%	up to +20.4%
	$\lambda = 70\%\lambda_{des}$	-17.3% & +45.8%	up to +37.4%
Synch, NS	$\lambda = \lambda_{des}$	-12.9% & +18.6%	up to +8.6%
	$\lambda = 90\%\lambda_{des}$	-14.6% & +21.5%	up to +11.0%
	$\lambda = 80\%\lambda_{des}$	-18.5% & +30.8%	up to +18.9%
	$\lambda = 70\%\lambda_{des}$	-24.0% & +46.9%	up to +33.9%
Asynch, PS	$\lambda = \lambda_{des}$	-9.6% & +15.5%	up to +9.3%
	$\lambda = 90\%\lambda_{des}$	-10.9% & +19.7%	up to +13.0%
	$\lambda = 80\%\lambda_{des}$	-14.1% & +30.9%	up to +23.7%
	$\lambda = 70\%\lambda_{des}$	-17.8% & +48.8%	up to +41.0%
Asynch, NS	$\lambda = \lambda_{des}$	-16.1% & +24.6%	up to +15.0%
	$\lambda = 90\%\lambda_{des}$	-16.9% & +28.3%	up to +17.2%
	$\lambda = 80\%\lambda_{des}$	-19.8% & +35.5%	up to +23.2%
	$\lambda = 70\%\lambda_{des}$	-23.7% & +48.0%	up to +36.3%

5.5 Uniformly distributed users

Another special case which illustrates the potential value of variable rate coding is the dependency of the optimal VRC & FRC throughput gains on the assumption that the users are Poisson distributed. In section 5.3, it was shown that synchronous FHMA systems with perfect side information, very accurate system loading statistics, Poisson distributed users, and optimal fixed rate coding could perform quite well compared to systems employing variable rate coding. In fact, with an RS code length of n=127, the peak normalized system throughput gain due to variable rate coding was only 5.2%. In this section we show that significant throughput gains due to variable rate coding are possible if the system loading statistics have a large variance in comparison to the Poisson distributed case.

If we consider the case where the users are uniformly distributed, we can model a system in which the loading statistics have a very high variance. If the system loading statistics have a high variance, then FRC systems become less effective since there is greater possibility for the optimal code rate (which would be used by a variable code rate system) to be much different than the fixed code rate.

In the case of uniformly distributed users in a synchronous perfect side information system, the expected normalized system throughput with an FRC scheme,

$$S_{fix}(\lambda) = \sum_{m=0}^{2\mu} \frac{1}{2\mu} \cdot \frac{R_{fix}(\mu) \cdot m}{q} \sum_{j=0}^{n-k} \begin{pmatrix} n \\ j \end{pmatrix} p_{h,m}(m)^j \cdot (1 - p_{h,m}(m))^{n-j}, \tag{5.32}$$

where $E[\cdot]$ is the expectation operator, $R_{fix}(\mu)$ is the fixed code rate which maximizes throughput when an average of μ users are present, and $p_M(m) = \frac{1}{2\mu}$ is the uniform distribution representing the probability of m users being present in the system where $0 \leq m \leq 2\mu$ [10].

[10] 2μ is the maximum number of users that can be in the system when there is an average of μ users in the system.

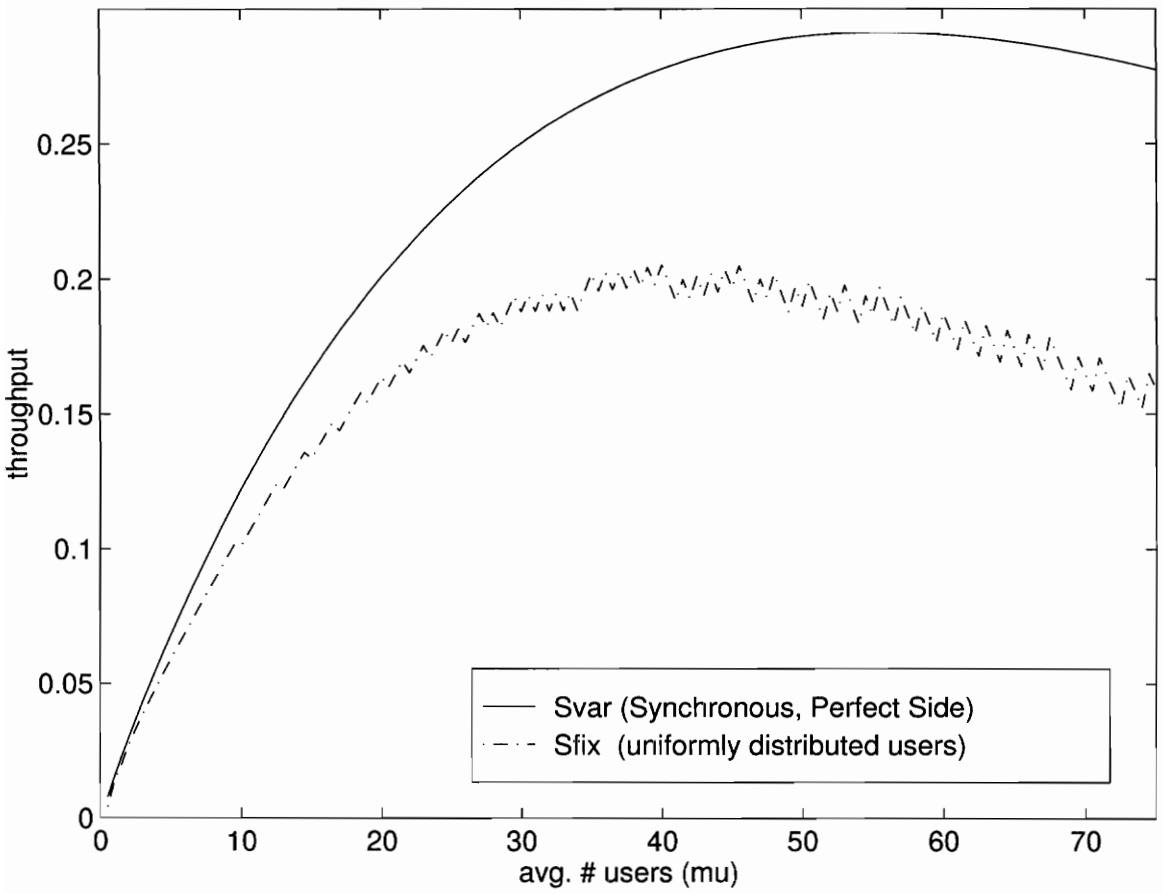

Figure 5.10: Throughput gains in a synchronous system with perfect side information, RS code length n=127, and Uniform distribution of users.

For a variable code rate system, the average expected normalized system throughput is

$$S_{var}(\lambda) = \sum_{m=0}^{2\mu} \frac{1}{2\mu} \cdot \frac{R_{var}(m) \cdot m}{q} \sum_{j=0}^{n-k} \binom{n}{j} p_{h,m}(m)^j \cdot (1 - p_{h,m}(m))^{n-j}, \tag{5.33}$$

where $R_{var}(m)$ is the variable code rate chosen to optimize $S_{var}(\lambda)$ for any given m.

From Figure 5.10 it is seen that with fixed rate coding, the peak normalized system throughput of 0.2054 occurs at an average loading of $\mu = 40$ users in the system. With variable rate coding, the peak normalized system throughput is 0.2912 and occurs at an average loading of $\mu = 56$ users. This represents a 41.8% gain in peak normalized system throughput (compared to a 5.2% gain in the Poisson distributed users case) and proves that significantly larger gains can be achieved in systems where the user distribution has a larger variance about the mean than the Poisson distribution.

Chapter 6
Conclusions

This thesis presented an analysis of the potential throughput benefits of employing a Variable Rate Coding (VRC) scheme in non-orthogonally hopped Frequency Hopped Multiple Access (FHMA) systems. The performance of VRC schemes for synchronous and asynchronous FHMA systems with and without collision information (i.e., side information) were analyzed and compared against the performance of optimal and realistic Fixed Rate Coding (FRC) schemes. Section 6.1 summarizes the key results of the analysis and section 6.2 discusses potential areas of future research in the area of Variable Rate Coding.

6.1 Summary of Key Results

The investigation of the benefits of spread spectrum systems (and in particular FHMA systems) began in chapter 2. Chapter 3 introduced error correction coding (or channel coding) as the primary means of combating "hits" in FHMA systems while chapter 4 introduced the concept of VRC as a means of increasing the capacity of a FHMA system by improving the coding efficiency.

6.1.1 Results for "Perfect Codes"

Sections 5.1 and 5.2 indicated that for perfect codes (i.e., codes that achieve channel capacity) an optimal VRC scheme can provide peak capacity improvements on the order of 21-35% when compared to optimal FRC schemes. From these results it is intuitive that the gains of a optimal VRC scheme against realistic (i.e., non-optimized) FRC schemes could be significantly higher than the 20-35% levels represented by the comparisons to optimal

FRC schemes. We explored the performance of the VRC and FRC schemes in a Rayleigh flat fading channel and found that the performance of the two schemes degraded identically with the throughput degradation in No Side information systems being more serious than in Perfect Side information systems. It was also shown that multiple access interference no longer dominates system performance apart from channel fading for E_b/N_o less than about 15 dB.

6.1.2 Results for Practical Length Reed-Solomon Codes

Section 5.3 indicated that optimal VRC schemes applied to FHMA systems employing Reed-Solomon (RS) block coding could achieve capacity gains of 3-10% for n=63 codes, 5-15% for n=127 codes, and 7-20% for n=255 codes when compared to optimal FRC schemes. We analyzed the performance of the Reed-Solomon VRC and FRC schemes in a Rayleigh flat fading channel and found that the two schemes degraded nearly identically in the fading channel with the VRC throughputs degrading slightly more than the FRC throughputs. Section 5.4 examined the throughput improvements of a VRC scheme compared to realistic (i.e., non-optimal) FRC schemes which are overdesigned to provide sufficient error correction capabilities for worst case channel conditions rather than average channel conditions. In the case of n=127 RS codes, it was shown that a VRC scheme can provide potential throughput improvements on the order of 35-40% when compared to an FRC scheme in which the actual system loading is 70% of the maximum design loading. These results suggested that potential throughput improvements provided by VRC can be significant for systems currently employing FRC schemes (which are overdesigned for average channel conditions). The sensitivity of the throughput gains provided by VRC to the accuracy of the estimates of the number of active users m was examined. Of the four system configurations examined, we found that the synchronous hopped system with perfect side information required the greatest accuracy in the estimates of m while the asynchronous hopped system with no side information tolerated the greatest amount of error in estimates of m. In the asynchronous hopped system with no side information it was found that if the estimates of m were within

-16% to +24% of the actual m ,then the VRC scheme provides superior performance over any FRC scheme (including an optimal FRC scheme).

6.2 Potential Areas of Future Research

The success of a VRC implementation in non-orthogonally hopped FHMA systems is highly dependent on the availability of estimates of the number of locally active users m. Thus one potential area of future research is in identifying and analyzing various methods of generating these estimates. An alternative to generating estimates of m by direct methods could be to use a "blind" estimation scheme where upon commencement of communication, the transmitter incrementally increases the transmission code rate from some nominal rate until the receiver measures that increasing throughput no longer occurs. From this information, it is possible to identify approximately where the throughput peak (and thus the optimal code rate $R_{var}(m)$) occurs. Research (possibly including simulation) into identifying robust algorithms which could be used for such a blind estimation scheme could be another area of future research in the application of VRC.

Although the analysis in this thesis focused on the application of VRC to non-orthogonally hopped FHMA systems, it is intuitive that VRC could hypothetically by applied to any system currently employing a FRC scheme (regardless of whether it is a wireless or wireline system). Therefore, the application of VRC to other types of systems (e.g., orthogonally hopped FHMA systems, DS/SS systems, narrowband systems, etc...) is another potential area of future research.

Chapter 7

Appendix

This appendix lists the source code routines used to generate and analyze the data presented in this thesis. The source code is executable in MATLAB, a software package available from The Math Works. The source programs used to generate results for each major section of this thesis is listed as well as the specific locations of these files. The program files can be found on the MPRG workstation network under the directory tree with root /andrew/vrc/.

7.1 Coding at Capacity: No Fading Results

7.1.1 Asynchronous hopping, No Side Information cases:

```
located in ~/andrew/vrc/Capacity/NoFading

For M=64 case run:
ANScapexact064.m
ANScaprandom064.m
ANSresults064.m

For M=128 case run:
ANScapexact128.m
ANScaprandom128.m
ANSresults128.m

For M=256 case run:
ANScapexact256.m
ANScaprandom256.m
ANSresults256.m
```

7.1.2 Asynchronous hopping, Perfect Side Information cases:

```
located in ~/andrew/vrc/Capacity/NoFading


For results for any M run:

APScapexact.m

APScaprandom.m
```

7.1.3 Synchronous hopping, No Side Information cases:

```
located in ~/andrew/vrc/Capacity/NoFading

For M=64 case run:
SNScapexact064.m
SNScaprandom064.m
SNSresults064.m

For M=128 case run:
SNScapexact128.m
SNScaprandom128.m
SNSresults128.m

For M=256 case run:
SNScapexact256.m
SNScaprandom256.m
SNSresults256.m
```

7.1.4 Synchronous hopping, Perfect Side Information cases:

located in ~/andrew/vrc/Capacity/NoFading

For results for any M run:

SPScaprandom.m

7.2 Coding at Capacity: Rayleigh Fading Results

7.2.1 Asynchronous hopping, No Side Information cases:

located in ~/andrew/vrc/Capacity/Fading

For M=128 case w/ binary FSK run:

ANScapexactM128FSK2.m

ANScaprandomM128FSK2.m

ANSresultsM128FSK2.m

7.2.2 Asynchronous hopping, Perfect Side Information cases:

```
located in ~/andrew/vrc/Capacity/Fading


For results for any M run:

APScapexactFSK2.m

APScaprandomFSK2.m

APScapresultsM128FSK2.m
```

7.2.3 Synchronous hopping, No Side Information cases:

```
located in ~/andrew/vrc/Capacity/Fading


For M=128 case run:

SNScapexactM128FSK2.m

SNScaprandomM128FSK2.m

SNSresultsM128FSK2.m
```

7.2.4 Synchronous hopping, Perfect Side Information cases:

```
located in ~/andrew/vrc/Capacity/Fading


For results for any M run:

SPScapexactFSK2.m

SPScaprandomFSK2.m

SPSresultsM128FSK2.m
```

7.3 Reed-Solomon Coding: No Fading Cases:

7.3.1 Asynchronous hopping, No Side Information cases:

```
located in ~/andrew/vrc/ReedSolomon/NoFading

For n=63 RS block codes:
ANS_RSexactN063.m
ANS_RSpoissonN063.m
optANS_RSexactN063.m
optANS_RSpoissonN063.m

For n=127 RS block codes:
ANS_RSexactN127.m
ANS_RSpoissonN127.m
optANS_RSexactN127.m
optANS_RSpoissonN127.m

For n=255 RS block codes:
ANS_RSexactN255.m
ANS_RSpoissonN255.m
optANS_RSexactN255.m
optANS_RSpoissonN255.m

For analysis of non-optimal FRC and VRC curves:
ANS_FRCbadestN127.m
ANS_VRCbadestN127.m
ANS_PLOTbadFRCest.m
ANS_PLOTbadVRCest.m
```

7.3.2 Asynchronous, Perfect Side Information cases:

```
located in ~/andrew/vrc/ReedSolomon/NoFading

For n=63 RS block codes:
APS_RSexactN063.m
APS_RSpoissonN063.m
optAPS_RSexactN063.m
optAPS_RSpoissonN063.m

For n=127 RS block codes:
APS_RSexactN127.m
APS_RSpoissonN127.m
optAPS_RSexactN127.m
optAPS_RSpoissonN127.m

For n=255 RS block codes:
APS_RSexactN255.m
APS_RSpoissonN255.m
optAPS_RSexactN255.m
optAPS_RSpoissonN255.m
```

7.3.3 Synchronous hopping, No Side Information cases:

```
located in ~/andrew/vrc/ReedSolomon/NoFading

For n=63 RS block codes:
SNS_RSexactN063.m
SNS_RSpoissonN063.m
optSNS_RSexactN063.m
optSNS_RSpoissonN063.m

For n=127 RS block codes:
SNS_RSexactN127.m
SNS_RSpoissonN127.m
optSNS_RSexactN127.m
optSNS_RSpoissonN127.m

For n=255 RS block codes:
SNS_RSexactN255.m
SNS_RSpoissonN255.m
optSNS_RSexactN255.m
optSNS_RSpoissonN255.m

For analysis of non-optimal FRC and VRC curves:
SNS_FRCbadestN127.m
SNS_VRCbadestN127.m
SNS_PLOTbadFRCest.m
SNS_PLOTbadVRCest.m
```

7.3.4 Synchronous hopping, Perfect Side Information cases:

```
located in ~/andrew/vrc/ReedSolomon/NoFading

For n=63 RS block codes:
SPS_RSexactN063.m
SPS_RSpoissonN063.m
optSPS_RSexactN063.m
optSPS_RSpoissonN063.m

For n=127 RS block codes:
SPS_RSn127.m (does all functions of the 4 separate scripts)

For n=255 RS block codes:
SPS_RSexactN255.m
SPS_RSpoissonN255.m
optSPS_RSexactN255.m
optSPS_RSpoissonN255.m

For analysis of non-optimal FRC and VRC curves:
SPS_FRCbadestN127.m
SPS_VRCbadestN127.m
SPS_PLOTbadFRCest.m
SPS_PLOTbadVRCest.m
```

7.3.5 Other Scripts Used by the Programs Above:

```
located in ~/andrew/vrc/ReedSolomon/NoFading


afhma2.m

afhma.m

afhmans2.m

afhmans.m

binomial.m

binomial2.m

fhma2.m

fhma.m

fhmans2.m

fhmans.m

poisson.m
```

7.4 Reed-Solomon Coding: Fading Cases (n=127 codes):

7.4.1 Asynchronous hopping, No Side Information cases:

located in ~/andrew/vrc/ReedSolomon/Fading

For n=127 RS block codes:

ANS_RSFexactN127.m

ANS_RSFpoissonN127.m

ANS_RSFresults_1.m

ANS_RSFresults_2.m

7.4.2 Asynchronous hopping, Perfect Side Information cases:

```
located in ~/andrew/vrc/ReedSolomon/Fading


For n=127 RS block codes:

APS_RSFexactN127.m

APS_RSFpoissonN127.m

APS_RSFresults_1.m

APS_RSFresults_2.m
```

7.4.3 Synchronous hopping, No Side Information cases:

```
located in ~/andrew/vrc/ReedSolomon/Fading


For n=127 RS block codes:

SNS_RSFexactN127.m

SNS_RSFpoissonN127.m

SNS_RSFresults_1.m

SNS_RSFresults_2.m
```

7.4.4 Synchronous hopping, Perfect Side Information cases:

```
located in ~/andrew/vrc/ReedSolomon/Fading


For n=127 RS block codes:

SPS_RSFexactN127.m

SPS_RSFpoissonN127.m

SPS_RSFresults_1.m

SPS_RSFresults_2.m
```

7.4.5 Other Scripts Used by the Programs Above:

```
located in ~/andrew/vrc/ReedSolomon/Fading


afhma2_RF.m
afhma_RF.m
afhmans2_RF.m
afhmans_RF.m
AllResults.m
binomial.m
binomial2.m
fhma2_RF.m
fhma_RF.m
fhmans2_RF.m
fhmans_RF.m
Plot.m
PlotFadingResults_2.m
poisson.m
r10dB.m
```

7.5 Uniformly Distributed Users Results:

located in ~/andrew/vrc/ReedSolomon/uniform

uniformfhma.m

optUniformN127.m

7.6 Latex and EPS files:

```
located in ~/andrew/vrc/latex

Latex files for final thesis draft:
fullthesis.tex
chapter1.tex
chapter2.tex
chapter3.tex
chapter4.tex
chapter5.tex
chapter6.tex
appendix.tex
biblio.tex

Latex files for MILCOM '95 paper:
fhma_mil.tex

Latex files for IEEE Transactions paper:
fhma.ieee2.tex

Associated Encapsulated Post Script (EPS) files for the Latex scripts above:
allpercent.eps
badestimates.30.percent.eps
badestimates.50.percent.eps
badVRCasynchNS.eps
badVRCasynchPS.eps
bincode.eps
```

cap.ne.synch.asynch.eps

cap.ps.synch.asynch.eps

capben.eps

capfading.eps

cdma.eps

chips.eps

conv.eps

despread.eps

fh2hits.eps

fh2users.eps

fhmamonitor.eps

fhmasys.eps

fhmasystempicture.eps

fhtx.eps

RS255.ns.synch.asynch.eps

RS255.ps.synch.asynch.eps

rdburst.eps

rscode.eps

RDfading.eps

sector3.eps

spread.eps

sstx.eps

uniform127gain.eps

uniquer.eps

vrc_vs_frc.eps

REFERENCES

[1] *Auction Fact Sheet*, F.C.C., http://www.fcc.gov/wtb/aucfct.html 1996.

[2] J.E. Padgett, C.G. Gunther, and T. Hattori, "Overview of wireless personal communications," *IEEE Communications Magazine*, vol. 33, no. 1, pp.28-41, Jan. 1995.

[3] D.C. Cox, "A radio system for widespread low-power tetherless communications," *IEEE Transactions on Communications*, vol. 39, no.2, pp.324-335, Feb. 1991.

[4] R.L. Pickholtz, D.L. Schilling, and L.B. Milstein, "Theory of Spread Spectrum Communications - A Tutorial", *IEEE Transactions on Communications*, Vol. COM-30, No. 5, pp. 855-884, May 1982.

[5] K.S. Gilhausen, et. al., "On the capacity of a cellular CDMA system", *IEEE Transactions on Vehicular Technology*, Vol. VT-40, No. 2, pp 303-312, May 1991.

[6] D.D. Falconer, F. Adachi, and B. Gudmundson, "Time Division Multiple Access Methods for Wireless Personal Communication, *IEEE Communications Magazine*, Vol. 33, No. 1, pp. 50-57, Jan 1995.

[7] F. de Seze, "Influence of Slow Frequency Hopping and Antenna Diversity Techniques in European GSM System", *Virginia Tech's fourth Symposium on Wireless Personal Communications*, Vol. 33, No. 1, pp. 15-1 to 15-10, June 1-3, 1994.

[8] D.L. Schilling, R.L. Pickholtz, and L.B. Milstein, "Spread Spectrum Goes Commercial", *IEEE Spectrum*, Aug 1989.

[9] P.D. Rasky et al., "Slow Frequency Hop TDMA/CDMA for Macrocellular Personal Communications," *IEEE Personal Communications Magazine*, pp. 26-35, Second Quarter 1994.

[10] J.C. Liberti, Jr. and T.S. Rappaport, "Analysis of CDMA Cellular Radio Systems Employing Adaptive Antennas," Dissertation for Ph.D. in Electrical Engineering at Virginia Tech, Blacksburg, VA., Sept. 1995.

[11] J.H. Winters, "Signal Acquisition and Tracking with Adaptive Arrays in the Digital Mobile Radio System IS-54 with Flat Fading," *IEEE Transactions on Vehicular Technology*, Vol. 42, No. 4, Nov. 1993.

[12] A. Kaul and B.D. Woerner, "An Adaptive Multistage Interference Cancellation Receiver for CDMA," Masters Thesis MPRG-TR-95-02 at Viginia Tech, Blacksburg, VA., March 23, 1995.

[13] A. Kaul and B.D. Woerner, "An analysis of adaptive multistage interference cancellation for CDMA," *Proceedings of the 45th IEEE Vehicular Technology Conference*, Rosemount, IL., July 26-28, 1995.

[14] S. Kim, *Coding for Spread Spectrum Communication Networks*, Dissertation for Ph.D. in Electrical Engineering and the University of Michigan, 1987.

[15] S. Kim and W. Stark, *Optimum Rate Reed-Solomon Codes for Frequency-Hop Spread Spectrum Multiple Access Communication Systems*, IEEE Transactions on Communications, Vol. 37, pp. 138-144, February 1989.

[16] A.I. Wardhana and B.D. Woerner, "Throughput of a FHMA System for Variable Rate Coding and Interference Estimates," Proceedings 1994 Tactical Communications Conference, Fort Wayne, IN, pp. 167-177, May 1994.

[17] R.A. Scholtz, "The Origins of Spread Spectrum Communications," *IEEE Transactions on Communications*, Vol. COM-30, no. 5, May 1982.

[18] J.G. Proakis, *Digital Communications*, McGraw-Hill, Inc., New York, NY, 1995.

[19] R.M. Buehrer and B.D. Woerner, *Spread Spectrum for Wireless Communications.*

[20] S.B. Wicker, *Error Control Systems for Digital Communication and Storage*, Prentice Hall, Englewood Cliffs, N.J., 1995, pp. 254-263.

[21] C.E. Shannon, "A Mathematical Theory and Communication," *Bell System Technical Journal*, vol. 27, July 1948, pp.3799-423, and Oct. 1948, pp. 623-656.

[22] C.E. Shannon, "Communication in the Presence of Noise," *Proceedings of the IRE*, vol. 37, Jan. 1949, pp.10-21.

[23] L.W. Couch II, *Digital and Analog Communication Systems*, Macmillan Publishing Company, New York, NY, 4th ed. 1993.

[24] X.L. Lin and B.D. Woerner, "Trellis-Coded Permutation Modulation for Improved Performance of Narrowband Noncoherent FSK," Masters Thesis MPRG-TR-96-15 at Virginia Polytechnic Institute and State University, May 17, 1996.

[25] T.S. Rappaport, *Wireless Communications Principles and Practice*, Prentice Hall Inc., 1995

[26] K. Cheun and W.E. Stark, "Probability of Error in Frequency Hop Spread Spectrum Multiple Access Communication Systems with Noncoherent Reception", *IEEE Transactions on Communications*, Vol. 39, No.9, pp. 1400-1410, Sept. 1991.

[27] Thomas M. Cover and Joy A. Thomas. *Elements of Information Theory.* John Wiley and Sons, Inc., New York, NY, 1991.

[28] E.A. Geraniotis and M.B. Pursley, "Error Probabilities for Slow Frequency Hopped Spread Spectrum Multiple Access Communications Over Fading Channels", *IEEE Transactions on Communications*, Vol. 30, No. 5, pp 996-1009, May 1982.

[29] G.D. Forney, "The Viterbi Algorithm", *Proceedings of the IEEE*, Vol. 61, pp 268-278, March 1973.

[30] M.V. Hedge and W.E. Stark, "Capacity of Frequency Hop Spread Spectrum Multiple Access Communication Systems", *IEEE Transactions on Communications*, Vol. 38, No. 7, pp 1050-1059, July 1990.

[31] M.B. Pursley and H.B. Russell, *Routing in Frequency-Hop Packet Radio Networks with Partial Band Jamming*, Proceedings 1990 Tactical Communications Conference, Fort Wayne, IN. pp. 117-126, April 1990.

[32] M.B. Pursley and H.B. Russell, *Network Protocols for Frequency-Hop Packet Radios with Decoder Side Information*, IEEE Journal on Selected Areas of Communications, Vol. 12, No. 4, pp. 612-621, May 1994.

[33] M.B. Pursley, *The Role of Spread-Spectrum in Packet Radio Networks*, Proceedings of the IEEE, Vol. 75, pp. 116-143, Jan. 1987.

[34] "Selecting a Wireless Local Area Network Technology," *Proxim Incorporated white paper*, http://www.proxim.com/proxim/apps/whiteppr/fh_vs_ds.htm.

[35] D.B. Brick and F.W. Ellersick, "Future Air Force Tactical Communications", *IEEE Transactions on Communications*, Vol COM-28, pp.1551-1572, Sept. 1980.

[36] R.M. Buehrer and B.D. Woerner, "The Application of Multiuser Detection To Cellular CDMA", , Dissertation for Ph.D. in Electrical Engineering at Virginia Polytechnic Institute and State University, June 27, 1996.

[37] D. Sweeney, *Virtual Wire – Smart Antennas*, Cellular Business, Vol. 13, No. 7, July 1996.

[38] J.L. Massey, "Shift Register Synthesis and BCH Decoding", *IEEE Transactions on Information Theory*, Vol IT-15, pp.122-127, Jan. 1969.

[39] E.R. Berlekamp, *Algebraic Coding Theory*, New York: McGraw-Hill, 1968 (rev. ed., Laguna Hills, Aegean Park Press, 1984).

VITA

Andrew S. Park was born in Platteville, Wisconsin on December 14, 1970. He received his Bachelor degree in Electrical Engineering from the Bradley Department of Electrical Engineering at Virginia Polytechnic Institute and State University in May 1994. He joined the Master of Science (M.S.) program in Electrical Engineering at Virginia Polytechnic Institute and State University in September 1994. Since then he has been a member of the Mobile and Portable Radio Research Group (MPRG) at Virginia Tech where he has been involved in research, simulation, and field testing of wireless communication systems for two and one half years. His research interests include Spread Spectrum, Channel Coding, Asynchronous Transfer Mode, and RF propagation.